



Published in final edited form as:

*Biomaterials*. 2020 March ; 233: 119591. doi:10.1016/j.biomaterials.2019.119591.

## Oral delivery of novel human IGF-1 bioencapsulated in lettuce cells promotes musculoskeletal cell proliferation, differentiation and diabetic fracture healing

J. Park<sup>a</sup>, G. Yan<sup>a</sup>, K.-C. Kwon<sup>a</sup>, M. Liu<sup>a</sup>, P.A. Gonnella<sup>a</sup>, S. Yang<sup>a,b,\*\*</sup>, H. Daniell<sup>a,\*</sup>

<sup>a</sup>Department of Basic and Translational Sciences, School of Dental Medicine, University of Pennsylvania, Philadelphia, PA 19104, USA

<sup>b</sup>The Penn Center for Musculoskeletal Disorders, School of Medicine, University of Pennsylvania, Philadelphia, PA 19104, USA

### Abstract

Human insulin-like growth factor-1 (IGF-1) plays important roles in development and regeneration of skeletal muscles and bones but requires daily injections or surgical implantation. Current clinical IGF-1 lacks e-peptide and is glycosylated, reducing functional efficacy. In this study, codon-optimized Pro-IGF-1 with e-peptide (fused to GM1 receptor binding protein CTB or cell penetrating peptide PTD) was expressed in lettuce chloroplasts to facilitate oral delivery. Pro-IGF-1 was expressed at high levels in the absence of the antibiotic resistance gene in lettuce chloroplasts and was maintained in subsequent generations. In lyophilized plant cells, Pro-IGF-1 maintained folding, assembly, stability and functionality up to 31 months, when stored at ambient temperature. CTB-Pro-IGF-1 stimulated proliferation of human oral keratinocytes, gingiva-derived mesenchymal stromal cells and mouse osteoblasts in a dose-dependent manner and promoted osteoblast differentiation through upregulation of ALP, OSX and RUNX2 genes. Mice orally gavaged with the lyophilized plant cells significantly increased IGF-1 levels in sera, skeletal

This is an open access article under the CC BY-NC-ND license (<http://creativecommons.org/licenses/by-nc-nd/4.0/>).

\*Corresponding author. Department of Basic and Translational Science, School of Dental Medicine, University of Pennsylvania, 240 South 40th St, 547 Levy Building, Philadelphia PA 19104-6030, USA. [hdaniell@upenn.edu](mailto:hdaniell@upenn.edu) (H. Daniell). \*\*Corresponding author. Department of Basic and Translational Science, School of Dental Medicine, University of Pennsylvania, 240 South 40th St, 437 Levy Building, Philadelphia PA 19104-6030, USA. [shuyingy@upenn.edu](mailto:shuyingy@upenn.edu) (S. Yang).

#### Author contributions

JP created and characterized all lettuce transplastomic lines expressing IGF-1 and evaluated efficacy in cell cultures and wrote relevant sections of original and revised manuscript. KCK codon-optimized Pro-IGF-1 created tobacco transplastomic lines and made marker-free chloroplast vector, wrote and edited these sections in the original and revised manuscript. PAG performed sera and muscle analysis, all oral gavage studies and wrote relevant sections of the original and revised manuscript. GY performed osteoblast in vitro study using IGF-1 provided by JP. GY, ML developed diabetes fracture mice, performed X-ray, Micro-CT, histological analysis and wrote relevant sections of the original manuscript. SY designed osteoblast differentiation, bone fracture and healing studies and wrote/edited relevant sections of the original manuscript. HD conceived this project, designed marker removal chloroplast vectors, strategies for screening excision of antibiotic resistance gene, evaluation of stability, different transmucosal delivery tags, creation/evaluation of transplastomic lines, long-term storage/stability, oral gavage strategies in animal studies, analyzed and interpreted data and wrote/edited original and revised versions of this manuscript.

#### Declaration of competing interest

The corresponding author is an inventor on several patents on expression of biopharmaceuticals in plants and his research was funded in the past by several major pharmaceutical companies including Bayer, Novo Nordisk, Johnson & Johnson and currently hemophilia research project is funded by Shire/Takeda. However, results presented here on IGF-1 is not funded by any industry or has no specific financial conflict of interest. All other authors do not report any conflict to report.

#### Appendix A.: Supplementary data

Supplementary data to this article can be found online at <https://doi.org/10.1016/j.biomaterials.2019.119591>.

muscles and was stable for several hours. When bioencapsulated CTB-Pro-IGF-1 was gavaged to femoral fractured diabetic mice, bone regeneration was significantly promoted with increase in bone volume, density and area. This novel delivery system should increase affordability and patient compliance, especially for treatment of musculoskeletal diseases.

### Keywords

Oral biopharmaceutical delivery; Human growth hormones; Bioencapsulation in plant cells; Musculoskeletal diseases; Chloroplast

---

## 1. Introduction

Forty years ago, recombinant human insulin was made in *E. coli* or yeast [1] and delivered through injections after purification. Although insulin pens or pumps have improved blood glucose monitoring or insulin delivery more precisely, needle-based delivery has been the only option for five decades. In addition, high cost of fermentation facilities, prohibitively expensive protein purification technologies, cold storage/transportation and sterile delivery make protein drugs unaffordable for a large global population earning < \$2/day. Indeed, top ten biologic drugs currently exceed 75% GDP of countries in the globe [2]. One approach to reduce cost of protein drugs is to express them in edible plant cells. However, glucocerebrosidase produced in carrot cells [3], approved by FDA in 2012 [4], failed to provide anticipated cost savings to Gaucher's disease patients when compared to other production systems such as CHO cells or human fibrosarcoma cells [5] due to the high cost of purification, the cold chain requirement, and injectable delivery.

In addition to the cost advantage, orally delivered therapeutic protein drugs (PDs) would be preferable to daily injections and could increase patient compliance, particularly for those patients who require long-term treatments such as muscle disorder, bone healing, or diabetes. PDs expressed in plant cells can be stored for several years at ambient temperature, after lyophilization, maintaining their efficacy [6,7]. Bioencapsulated PDs in plant cells are protected by the plant cell wall from digestive enzymes and acidic pH. They can be released into the circulatory system and delivered to target cells or tissues when gut bacteria lyse the plant cell wall and PDs enter intestinal epithelial cells via endocytosis or pinocytosis depending on fused tags [Cholera non-toxic B subunit (CTB) or protein transduction domain (PTD)] [2,8]. This natural process eliminates the need for prohibitively expensive fermentation, purification, and cold storage/transportation [2,9]. Although the attempt to orally deliver glucocerebrosidase made in carrot cells was not successful [3] due to lower levels of expression, in a landmark clinical trial, orally delivered low doses of peanut antigens in plant cells showed that allergy can be suppressed and FDA approval is anticipated very soon [10]. This plant cell-based oral delivery approach has opened the door for the clinical applications of proteins made in plant cells. The released antigens can modulate the gut immune system to treat a number of allergies and suppress antibodies against injected protein drugs, which frequently happens in enzyme replacement therapies [2,8,9]. In this study, we explore repetitive long-term oral delivery of a protein drug using

human Insulin-like growth factor (IGF-1) as a novel therapeutic PD for musculoskeletal diseases.

IGF-1, upon binding to the IGF-1 receptor, is a major player in skeletal muscle and bone development, growth, and maintenance of physiological strength. This growth factor can directly enhance muscle mass and bone density [11]. Treatment of myotonic dystrophy type 1 patients with IGF-1/IGF-1 binding protein complex via subcutaneous injections for 24 weeks increased body mass and metabolism [12]. While conditional deletion of IGF-1 in collagen type 1 alpha 2-expressing cells reduces osteoblast number, activity and bone mass in mice [13], overexpression of IGF-1 increased bone volume and remodeling [14]. In addition, lower IGF-1 levels in serum have been suggested to be associated with an increased risk of fractures [15,16]. Local delivery of IGF-1 accelerates bone formation in a rat fracture healing model [17] and IGF-1 administration in patients increased bone healing, with rapid clinical improvements with hip or tibial fractures during osteoporosis [18]. Interestingly, decreased levels of IGF-1 both in serum and in fracture region have been reported in diabetic rat, which has been suggested to be one of the reasons for defective bone healing or delayed union [19]. Moreover, IGF-1 facilitates survival, proliferation, differentiation in bone-resorbing osteoclasts and bone-forming osteoblasts. A previous study showed that decreased circulating IGF-1 resulted in reduction of bone density [20]. IGF-1 also regulates tooth root development and root dentin stem cells. Exogenous IGF-1 stimulated proliferation and differentiation of isolated human tooth root stem cells [21]. Aforementioned roles of IGF-1 in proliferation/differentiation of satellite cells leading to muscle generation, together with bone growth/remodeling including dental root development can enhance its potential as a therapeutic for multiple musculoskeletal disorders.

IGF-1 is present in three forms in the extracellular matrix: precursor IGF-1 which retains e-peptide (Pro-IGF-1), Pro-IGF-1 with N-glycosylation (Gly-Pro-IGF-1), and mature IGF-1 [22]. Due to its retention, potential biological activities of e-peptide have emerged for either the e-peptide alone or for the precursor. Pro-IGF-1 with e-peptide demonstrated positive effects for muscle disorders treatment and increased binding to IGF-1R than mature IGF-1, whereas Gly-Pro-IGF-1 showed less efficiency at IGF-1R activation [23]. IGF-1 in clinical trials for muscle therapy is delivered via daily subcutaneous injections lacking e-peptide but with e-peptide, its functional efficiency could be increased ([clinicaltrials.gov/ct2/show/NCT01207908](https://clinicaltrials.gov/ct2/show/NCT01207908), [24]). Previous studies suggested potential biological roles of e-peptide. Pro-IGF-1 and Gly-Pro-IGF-1 are predominant rather than mature IGF-1 in skeletal muscles and this proportion was maintained even after viral over-expression of the *Igf1* gene. The e-peptide requirement for muscle mass was proposed based on lack of improvement on muscle hypertrophy in young mice after over-expression of IGF-1 [25] and increased phosphorylation of cascade proteins was shown when Pro-IGF-1 was virally over-expressed [22]. Moreover, independent e-peptide has stimulated IGF-1R signaling and regulated cell proliferation and differentiation in various human cells and cell lines [22]. Therefore, the retention of e-peptide in Pro-IGF-1 expressed in chloroplasts will be conducive to improve efficacy of IGF-1 currently used in the clinic.

In addition to developing a novel IGF1, we address several limitations of previous studies on oral delivery of PDs using IGF-1. The low level expression that led to inadequate delivery of

PDs is addressed through expression in chloroplasts, up to 10,000 copies of foreign genes in each plant cell, which is the highest copy number feasible in any protein bioreactor [2,8,26–28]. In addition, chloroplasts are ideal for several post-translational modifications including disulfide bonds required for proper folding and functionality of biopharmaceuticals [27,28]. Another limitation is presence of antibiotic resistance genes in genetically modified cells. Although genetically modified soybean and corn containing antibiotic resistance genes have been approved by FDA and consumed by billions of people around the globe in the past three decades, the higher copy number used to enhance expression in chloroplasts may pose some hurdles, even when drugs are delivered infrequently when compared to daily consumption of GM food. Previous studies have reported IGF-1 expression in seeds [29], non-edible plants [30] or cell cultures [31] but a precursor form of IGF-1, Pro-IGF-1 retaining e-peptide, has never been expressed or functionality evaluated in suitable animal models upon oral delivery. Bone morphogenetic protein 2 expression failed in lettuce chloroplasts but was expressed via the nuclear genome. However, no fusion tag for transmucosal delivery was used for evaluation of oral delivery [32].

Therefore, in this study, we created plants expressing codon optimized Pro-IGF-1 containing the e-peptide fused with transmucosal carriers Cholera non-toxic B subunit (CTB) or cell penetrating protein transduction domain (PTD) in chloroplasts. Most importantly, we deleted the antibiotic resistance gene, evaluated transgene stability in subsequent generations of plants, efficacy in proliferation or differentiation of different human/mouse oral cells, oral delivery to the circulatory system and muscle, and bone healing in a diabetic fracture mouse model. Together with the complete removal of the antibiotic resistance gene, this novel platform should facilitate clinical studies of bioencapsulated biopharmaceuticals for affordable oral drug delivery and enhanced patient compliance.

## 2. Results

### 2.1. Generation of lettuce/tobacco transplastomic lines expressing CTB-Pro-IGF-1

Tobacco and lettuce systems were used to evaluate expression because the former is known for three decades whereas the edible lettuce is an emerging new system with only a few therapeutic proteins expressed so far. Furthermore, selectable marker removal has been so far reported only in tobacco chloroplast genomes and no antibiotic free therapeutic protein has been reported in an edible crop. The precursor form of human IGF-1 with e-peptide (Pro-IGF-1) was synthesized after codon optimization to improve its expression level in chloroplasts, based on the codon usage hierarchy analyzed using highly expressed *psbA* gene sequences from 133 plant species [33]. Out of a total 105 codons of Pro-IGF-1, 65 codons were optimized resulting in increased AT content from 43% to 57%. In addition, three amino acids were changed (K68G, R74A, and R77A) to avoid the recognition by endoprotease so as to prevent e-peptide cleavage [34] (Fig. S1 and Table S1). In a previous study, mutations of Pro-IGF-1 on the prohormone processing and predicted glycosylation sites increased proportion of non-glycosylated Pro-IGF-1 without losing activity to IGF-1R [23]. However, the predicted glycosylated sites were not edited in this study because it is well known that the chloroplast is a glycosylation free zone and it offers protection from glycosylation even with potential glycosylated sites.

The codon optimized Pro-IGF-1 was fused to CTB via a hinge (GPGP) and a furin cleavage (KKRKS<sub>V</sub>) sequence [35], and the fusion construct was cloned into the lettuce (pLsLF) (Fig. 1A) or tobacco (pLD-utr) chloroplast transformation vectors (Fig. 1E). After bombardments of the plasmids to lettuce/tobacco leaves, shoots regenerated after the first round of selection were tested using PCR analysis with specific primer sets (Fig. 1A and E) to confirm site specific integration of the expression cassettes (Fig. 1B). PCR-positive shoots were subjected to another round of selection to achieve homoplasmy. The homoplasmic states were confirmed by Southern blots using suitable probes (SB-P) (Fig. 1C and F) and expression of CTB-Pro-IGF-1 was detected in western blots (Fig. 1D). The transformed chloroplast genomes showed distinct fragments of 11.6 kb (Fig. 1C) or 6.7 kb (Fig. 1F) in lettuce or tobacco, respectively, confirming the integration of the CTB-Pro-IGF-1 expression cassettes when compared to smaller fragments in the untransformed chloroplast genomes (9.1 kb (Fig. 1C) or 4.4 kb (Fig. 1F) in lettuce or tobacco, respectively). The western blot showed expression of CTB-Pro-IGF-1 protein of the expected size (24.3 kDa) (Fig. 1D). These results confirmed the generation of lettuce/tobacco homoplasmic lines expressing CTB-Pro-IGF-1.

## 2.2. Generation of marker-free PTD-Pro-IGF-1 homoplasmic lettuce lines

The marker-free chloroplast vector (pLsLF-MF) was generated by multiple cloning steps (Fig. S2) containing the spectinomycin resistant aminoglycoside-3'-adenylyl-transferase (*aadA*) gene under the control of plastid ribosomal RNA promoter (*Prrn*) and 3' UTR (*TrbcL*). The *aadA* is inserted between two copies of chloroplast encoded CF1 ATP synthase subunit beta (*atpB*) promoter region (649 bp) as shown in Fig. 2A. The codon-optimized synthetic Pro-IGF-1 fused to PTD via the hinge and furin sequence was cloned into the marker-free chloroplast expression cassette, under the control of the *psbA* promoter/5' UTR and 3' UTR. The bombarded lettuce leaves were regenerated on spectinomycin containing media and subsequently screened with specific sets of PCR primers during the first (data not shown) and second round of selections (Fig. 2B). The 16s-F/*aadA*-R primer set anneals to the endogenous chloroplast genome sequence and the *aadA* transgene within the cassette (Fig. 2A), which amplified a 3.3 kb DNA fragment (Fig. 2B). The set of UTR-F/23s-R primers was used to verify 3' region of the expression cassette (Fig. 2A), which produced a fragment of 2.4 kb (Fig. 2B).

During the selection of lettuce chloroplast transformants on spectinomycin, the selection marker is excised, leaving one copy of the *atpB* region in the transplastomic genome by homologous recombination between the two directly repeated *atpB* fragments. Upon marker gene excision, the primer set of 16s-F/*atpB*-R should amplify a 2.4 kb PCR product and the 16s-F/*aadA*-R should not produce any PCR products. As shown in Fig. 2B, transplastomic line 1 showed no PCR product when amplified with the 16s-F/*aadA*-R primer set, resulting from the excision of the *aadA* gene, with the presence of an amplified 2.4 kb fragment by the 16s-F/*atpB*-R. This excision didn't affect the stable integration of the PTD-IGF-1 expression cassette, which was confirmed by the PCR amplification of a 2.4 kb fragment using the UTR-F/23s-R primer set. In lines 2, 3, and 4, 3.3 kb PCR products were produced by the 16s-F/*aadA*-R, indicating that the *aadA* marker gene was still present in the chloroplast genomes (Fig. 2B). Three primary shoots showed positive results in the

1st PCR screening; among 9 shoots screened in the 2nd round of selection, 6 shoots were positive for transgene cassette integrations and one shoot showed complete removal of the *aadA* gene.

The PCR positive shoots (line 2, 3 and 4) in Fig. 2B were examined along with the antibiotic resistance gene-free shoot (line 1) and untransformed wild type lettuce by Southern blot analysis (Fig. 2C). In the Southern blot, while untransformed lettuce showed a single 9.1 kb fragment, transplastomic line 1 showed a 10.7 kb fragment supporting the PCR results (Fig. 2B) and achievement of homoplasmic marker-free line (marker gene excision from all copies of the chloroplast genome). Interestingly, in line 2, 3, and 4, two fragments at 12.7 kb and 10.7 kb in sizes were detected, which represents a heteroplasmic state with or without the marker excision. Regardless of the *aadA* gene excision, expression of PTD-Pro-IGF-1 protein was detected at the expected size, 14.5 kDa, in all the examined lines when using IGF-1 antibody, while no band was detected in the untransformed wild type lettuce (Fig. 2D).

To evaluate stability of the marker-free homoplasmic status in the next generation, 10 marker-free seeds were germinated on spectinomycin-free media. Genomic DNA PCR with the same primer sets used in T0 transplastomic line and Southern blots were carried out (Fig. 2E and F). All the examined seedlings showed the excision of antibiotic resistance gene but maintained the integration of the PTD-Pro-IGF-1 expression cassette. Expression of PTD-Pro-IGF-1 in the T1 generation was also confirmed by western blots against anti-IGF-1 (Fig. 2G). As shown in the T0 plants (Fig. 2D), all examined T1 plants expressed PTD-Pro-IGF-1 after the marker gene excision. Also, when T1 marker-free transplastomic lines were germinated on antibiotic containing media (spectinomycin 25 and 50 µg/mL), the leaves bleached out in 6 days after germination and the plants stopped growing 15 days after germination (Fig. S3). Randomly selected 4 lines of T2 marker-free plants also showed the antibiotic resistance gene-free homoplasmic state expressing Pro-IGF-1, as confirmed by Southern blot and immunoblot analysis, respectively (Fig. 2H and I). These data confirm that the marker-free state is stably maintained through subsequent T1 and T2 generations, while maintaining expression of Pro-IGF-1.

### 2.3. Characterization of CTB/PTD-Pro-IGF-1 expression in lyophilized plant cells

Expression of CTB-Pro-IGF-1 in both lettuce (Fig. 3A and B) and tobacco (Fig. 3C and D) chloroplasts was evaluated using antibodies against CTB or IGF-1. The two different antibodies detected the same size of the target protein. Based on a standard curve generated using known amounts of IGF-1 peptide, a concentration of expressed PTD-Pro-IGF-1 in lyophilized lettuce leaves was 270 µg/g dry weight (Fig. 3E). Likewise, using a CTB standard curve, CTB-Pro-IGF-1 concentration was 370 µg/g in lyophilized lettuce T0 lines (data not shown). Concentrations of the expressed therapeutic protein were compared between fresh and lyophilized cells using immunoblot analysis with antibodies against CTB or IGF-1 (Fig. 3F and G). Concentrations of both CTB- and PTD-Pro-IGF-1 were ~10-fold higher in the lyophilized samples when compared to those in fresh leaves based on weight. Such increase in concentration based on weight is due to removal of water and this is not specific to IGF-1 but is observed in all quantified plant proteins.

Harvested fresh leaves were frozen and stored at  $-80^{\circ}\text{C}$ , and the frozen leaves underwent a 3-day sublimation process at low atmospheric pressure (400 mTorr) with gradual temperature change (from  $-40^{\circ}\text{C}$  to  $25^{\circ}\text{C}$ ) to remove solid water molecules adhering to proteins, without any loss of biological activity. Since lyophilization only removes the solid water molecules attached to the frozen proteins, the same protein profile is observed in western blots in fresh and lyophilized samples (Fig. 3 F and G). The pentameric form of CTB, which is created by disulfide bonds, 30 hydrogen bonds, 7 salt bridges and several hydrophobic interactions among CTB monomers, can bind to GM1 receptor [36]. CTB carries any fused proteins across gut epithelial cells by binding to GM1 receptors, so that the fused proteins can be delivered to the circulatory system when cleaved off from the CTB by the ubiquitous protease furin [8]. To investigate formation of the pentameric CTB structure, GM1 binding ELISA was performed using fresh or lyophilized lettuce (Fig. 3H) or tobacco (Fig. 3I) leaves expressing CTB-Pro-IGF-1. The absorbance values of the fresh and lyophilized cells expressing the CTB fusion proteins at 450 nm were as high as the CTB standard proteins (positive control), with no significant signal in negative controls. These results show that the expressed CTB-Pro-IGF-1 in chloroplasts can be properly folded in the pentameric form and the integrity of the pentameric structure can be also maintained after lyophilization. It should be noted that GM1 ELISA performed in this study is a qualitative assay and not quantitative, because pentamers form aggregates in plant extracts. Therefore, quantitation to determine drug dose is done using western blots. The presence of the pentameric CTB-Pro-IGF-1 structures in the tobacco lyophilized cells further confirmed using non-reducing SDS-PAGE (Fig. 3J). The size of the pentameric form of CTB-Pro-IGF-1 is  $\sim 121.5$  kDa but a larger size was observed, which is probably a dimer form of the pentameric structure. This may be due to the strong interactions between CTB pentamers in absence of reducing agents [36] and/or inter or intra molecular disulfide bonds in IGF-1 [27]. Most importantly, the single protein band in Fig. 3J supports existence of only the assembled CTB-Pro-IGF-1 pentamers in plant cells and absence of any cleaved products shows remarkable stability.

Expression levels of Pro-IGF-1 in the transplastomic lines were significantly increased in the next generation (Fig. 3K and 3L). The levels of both CTB-Pro-IGF-1 or PTD-Pro-IGF-1 were higher in T1 lines than those of T0 lines, with an average of 15-fold in CTB- and 7-fold in PTD-Pro-IGF-1, irrespective of the marker removal or the fusion tag. Expression levels of Pro-IGF-1 were stable up to 31 months (Fig 3 M, N, O) in lyophilized plant cells. No significant change in IGF-1 level was observed in the lyophilized powder (IGF-1  $\mu\text{g/g}$  Dry Weight) during long-term storage, with an average of 370  $\mu\text{g/g}$  of CTB- and 270  $\mu\text{g/g}$  of PTD-Pro-IGF-1, when the same batch of plant powder was examined in western blots at different storage time points, regardless of the selectable marker excision. Evaluation of lyophilized plant cells stored for 1–20 months showed similar folding and assembly of the CTB pentamer structures for GM1 receptor binding efficacy, irrespective of long-term storage duration (Fig. 3H and I). The expression of IGF-1 didn't impact plant growth or fertility probably because plants do not have IGF-1 receptors or IGF-1 signaling pathways.

#### 2.4. Cell proliferation induced by chloroplast expressed CTB-Pro-IGF-1

To evaluate cell proliferation effects of the plant derived CTB-Pro-IGF-1 in vitro, MTT assay was performed on four different human and mouse cell types: HOK (Human Oral Keratinocytes), GMSCs (Human Gingiva-derived Mesenchymal Stromal Cells), SCCs (Human head and neck Squamous Carcinoma Cells), and mouse osteoblasts (MC3T3). CTB-Pro-IGF-1 was purified from lyophilized plant cells, due to higher concentration than in fresh plant cells (Fig. 3 F and G), using the affinity of nickel binding to histidine residues when CTB monomers form the pentameric CTB-Pro-IGF-1 structures (Fig. S4). After the purified chloroplast derived protein was evaluated by immunoblot analysis with a commercial human mature IGF-1 peptide, different concentrations of CTB-Pro-IGF-1 were tested in four different oral cell types. The chloroplast derived CTB-Pro-IGF-1 stimulated proliferation of HOK (~1.2-fold), GMSCs (~1.7-fold) and mouse osteoblasts (~1.7-fold) when compared to the commercial IGF-1 (Fig. 4A, B, and 4D), while similar effects on proliferation was observed in SCCs (Fig. 4C). These results demonstrate that the plant derived human IGF-1 with e-peptide promotes cell proliferation in a dose dependent manner. Cell proliferation rate is higher on HOK, GMSCs, and mouse osteoblasts, indicating the human Pro-IGF-1 expressed in plant chloroplasts is fully functional and more effective than the currently used mature IGF-1 product in the clinic. The recombinant Pro-IGF-1 can be superior to the clinical IGF-1 due to the retention of the e-peptide, stabilized by three point mutations made in the endoprotease recognition site to prevent its cleavage, confirming the importance of e-peptide in growth and repair. To determine whether the plant derived Pro-IGF-1 can promote osteoblast differentiation, MC3T3 cells were incubated in OS medium with or without purified CTB-Pro-IGF-1 for 5 days and expression levels of osteogenesis markers (ALP, OSX, RUNX2) were examined. Our data showed that treatment with CTB-Pro-IGF-1 at 300 ng/ml significantly up-regulated the expression of ALP, OSX, and RUNX2, demonstrating that the plant derived Pro-IGF-1 can promote osteoblast differentiation along with proliferation (Fig. 4E).

#### 2.5. Evaluation of IGF-1 levels after oral delivery

We orally gavaged Pro-IGF-1 expressed in chloroplasts of tobacco, lettuce with marker, and lettuce without marker to evaluate IGF-1 levels in sera and muscles after their oral delivery. Our results show efficient delivery of all three plant products to the sera of C57BL6/J mice (Fig. 5A). Baseline values of 4.3 ng/ml  $\pm$  1.35 (SEM) of circulating IGF-1 were increased by 2 h–10.6 ng/ml  $\pm$  1.6 (SEM) in the sera of mice fed with CTB-Pro-IGF-1 lyophilized tobacco plant powder (5  $\mu$ g IGF-1). Likewise, CTB-Pro-IGF-1 produced in lettuce also increased from a baseline of 3.9 ng/ml  $\pm$  0.61 (SEM) to 11.62 ng/ml  $\pm$  1.9 (SEM), with a 5  $\mu$ g dose of IGF-1. These results show similar absorption levels from both plant products utilizing CTB for transport via the GM1 receptors. When PTD-Pro IGF-1, which utilizes macropinocytosis for penetration of the epithelial barrier was tested, similar absorption efficacy was observed. Increases from baseline values of 2.8 ng/ml  $\pm$  0.5 (SEM) to 8.1 ng/ml  $\pm$  1.5 (SEM) in gavaged mice were found. No significant differences between males and females were observed. Within each group, some differences in bioavailability were seen but we observed 2-3-fold increase on an average in all gavaged groups. These results demonstrate that PTD-Pro-IGF-1 produced in transplastomic plants, that lack the antibiotic resistance gene, can be orally delivered via an endocytic mechanism.

We conducted pharmacokinetic experiments in mice for quantification of IGF-1 in sera following oral gavage (Fig. 5B). IGF-1 levels were measured at 2, 6, 8, and 24 h. At 2 h, IGF-1 showed a 39% increase over baseline (0 h), declined to 35% at 6 h, 8% at 8 h and slowly returned to baseline levels after 24 h. As explained above, release of Pro-IGF-1 in the gut lumen depends on gut microbial enzymes capable of digesting the plant cell wall. Very few gut bacterial species capable of releasing enzymes have been characterized and further research is needed to characterize their role. However, we could examine the effectiveness of cell wall-degrading enzymes produced by gut microbes to release Pro-IGF-1 from the plant cells in vitro (Fig. 5C). Four digestive enzymes present in the gastrointestinal tract (mannanase, pectinate lyase, endoglucanase and exoglucanase) were expressed in plant cells. PTD-Pro-IGF-1 expressing lyophilized plant cells (10 mg) were incubated in vitro in the presence or absence of a mixture of plant cell wall degrading enzymes expressed in plant cells [37,38]. After 2 h incubation at room temperature, an increase of IGF1 from  $7 \pm 2$  ng/ml in the absence of enzymes to  $27 \pm 1$  ng/ml in the presence of enzymes, providing further insight into the mechanism of drug release in the gut lumen.

Furthermore, the presence of increased IGF-1 in gastrocnemius (Fig. 5D) and soleus muscle (Fig. 5E) at 5 h after the oral gavage indicates that CTB and PTD act as transmucosal carriers for the delivery of IGF-1 to muscle tissues. IGF-1 was increased in both gastrocnemius and soleus muscle ~28% at 5 h after feeding (Fig. 5D and E), indicating that CTB or PTD-Pro-IGF-1 can be efficiently delivered into different muscle tissues. Although the plant cells were gavaged after storage for 4, 6, 31 months (due to creation of the transplastomic lines at different time points), the gavaged Pro-IGF-1 in all three plant cells increased IGF-1 levels in sera 2.5- to 3 fold, regardless of duration of storage, confirming their functionality after prolonged storage as lyophilized powder. This unique advantage eliminated the need for cold storage and transportation of protein drugs currently used in the clinic.

## 2.6. Systemic administration of IGF-1 promotes bone regeneration in diabetic fracture model

To further characterize the effect of CTB-Pro-IGF-1 in vivo in a disease model, we chose to use fracture models in both Diabetes (Dia) and age/gender matched non-diabetes wild type (CON) mice. Micro-CT images, which covered around 3 mm proximal and 3 mm distal to the fracture sites, were acquired at 6 weeks post-fracture. As expected, 3D reconstruction of microCT images showed a significant reduction of bone formation in Dia mice compared to that in CON mice. Dia mice had much less bone mass with low-bone density and porous woven bone in the fracture sites compared to CON mice (Fig. 6A). Accordingly, ratio of BV/TV (bone volume fraction) and bone connectivity density were decreased by 54% and 39% respectively. Moreover, histological analysis results showed that relative bone area was reduced by 31% in Dia mice when compared to CON mice (Fig. 6B). The bone volume, density and area were significantly increased after IGF-1 treatment when compared to WT plant treated Dia mice (Fig. 6). This demonstrates that the orally delivered CTB-Pro-IGF-1 can effectively restore bone healing of diabetic fracture.

### 3. Discussion

IGF-1 has been used as a therapeutic candidate to treat multiple muscle disorders. Circulating IGF-1 produced mostly in the liver is not adequate to improve muscle hypertrophy, therefore delivery to muscle tissue is required for efficacy. Boosting IGF-1 levels in the circulatory system is a suitable strategy since elevated IGF-1 levels in sera resulted in muscle mass enhancement due to their trans-localization to the muscle tissues [24]. It is well established that oral administration of untagged IGF-1 results in little or no-detectable IGF-1 in sera. Therefore IGF-1 has been administered by injections in clinical studies. No detectable IGF-1 was found in sera of pigs fed 3.4 mg/kg IGF-1 per day for four days [39]. Recombinant IGF-1 was increased in serum levels in humans approximately 100% over 20 days of 12 hourly injections in malnourished CAPD patients [40]. In contrast, the present study demonstrates that orally delivered Pro-IGF-1 raised circulating levels of IGF-1–100% at 2 h and ~28% increases in local muscle tissues at 5 h after a single dose in mice.

We compared increases in IGF-1 in sera and muscles between PTD-Pro-IGF-1 and CTB-Pro-IGF-1 fed mice to distinguish efficiency of non-receptor mediated vs. receptor-mediated delivery. We observed ~28% increases of IGF-1 in muscle tissues for both PTD-Pro-IGF-1 and CTB-Pro-IGF-1 fed mice. In contrast to the receptor-mediated transport of proteins fused with CTB, PTD penetrates cell membranes by stimulating macro-pinocytosis and does not enter immune modulatory cells [41]. The ability to deliver Pro-IGF-1 to muscle tissue using PTD presents an unique advantage in drug delivery for prevention of antibody development, which is often a challenge for several injected protein drugs in hemophilia or other diseases [2,7].

Several mechanistic observations could be made based on these results. First, the bioencapsulation of IGF-1 within plant cells protects Pro-IGF-1 from the digestive enzymes or extremely acidic pH in the stomach. Plant cell walls have  $\beta$ -1,4 and  $\beta$ -1,6 linkages, which can't be hydrolyzed by human digestive enzymes [42]. Intact plant cells also prevent acid hydrolysis of bioencapsulated proteins. Based on these concepts, intact plant cells containing protein drugs, ranging from very small regulatory proteins (Ang1-7 [43,44], exendin [45], or insulin [46]) to very large proteins [6,47–50] or vaccine antigens [51–60] have been delivered to the circulation or immune system demonstrating their protection from acids and enzymes. Indeed, such protection was visually demonstrated using lyophilized plant cells expressing CTB-GFP; GFP fluorescence in intact cells was observed first nearby villi and then GFP was observed inside gut epithelial M cells [35,41], which shows that GFP fused with CTB or PTD was taken up via endocytosis or pinocytosis pathways, after their release from plant cells in the gut lumen. The cellulolytic bacteria are closely associated with the plant cell surface, forming a biofilm and colonizing the gut mucus [42]. This biofilm provides another layer of protection for the protein drugs from intestinal proteases in the gut lumen. In this study, we have provided further insight into this process by demonstrating release of Pro-IGF1 from intact plant cells after incubation with cell wall degrading enzymes released by commensal bacteria. Released CTB fused protein drugs bind to GM1 receptors present on epithelial cell surface. GM1 is highly abundant - 15,000 per cell [61] and the average surface area of the intestine is ~32 m<sup>2</sup> [62]. Irrespective of fusion tags used, GFP

is very efficiently delivered to the liver. Biodistribution to the liver is higher than any other tissues because blood carries proteins from the gut to the liver via the portal vein [41]. GFP studies show that liver takes up orally delivered proteins to a level of saturation that is not dependent on the fusion tag.

Second, both transmucosal carriers (CTB, PTD) are equally efficient in delivering IGF-1 into circulation, even though they use very different mechanisms to cross the gut epithelial cells [41]. Third, furin is a ubiquitous protease presents in most cells and tissues [8]. It cleaved off the fused tags from Pro-IGF-1 producing the same size of proteins as endogenous IGF-1 based on the detected IGF-1 in the muscle tissues after the oral gavage, which confirms efficiency of the engineered furin cleavage site. Release of fused proteins without CTB into the circulation after the furin cleavage or lack of protein delivery without transmucosal carriers have been reported in previous studies [35,63]. As stated above, no detectable IGF-1 was found in sera of pigs fed with very high doses 3.4 mg/kg IGF-1 per day for four days [39].

Differences observed in bioavailability in individual animals within the same group using the same tag (CTB or PTD) are most likely due to variability in the number of plant cells gavaged because plant cells were resuspended in PBS and gavaged using a needle. The needle based oral delivery is not relevant to the clinic but is the only option available for mice. In addition, food was not withdrawn from cages to fast the animals before the oral gavage, in order to simulate natural drug delivery conditions, as in the clinic. Therefore, there is some variability in the digestion rate of the plant cells containing IGF-1. Several previous studies have reported efficacy of dose-dependent delivery upon oral administration of large blood clotting factor proteins, including FIX [6,7] or FVIII [47]. Because these studies were done in different animal models (mice, dogs) for different durations (3–12 months) using different diets or at different locations (Florida, North Carolina, Indiana, Pennsylvania), there is no evidence to indicate that variation in gut microbes significantly impacts the delivery of drugs bioencapsulated in plant cells. Delivery of only the fusion tag as control without IGF-1 was not tested because of difficulty in expression of PTD alone (4 kDa) or numerous prior studies using CTB alone as a vaccine antigen [8,52] or CTB with a reporter protein like CTB-GFP [35]. The oral administration of IGF-1 is preferable to daily injections, which are necessary in patients due to the 12-h half-life of IGF-1 in blood [64]. These findings indicate that the chloroplast derived Pro-IGF-1 could be an effective approach to treat musculoskeletal disorders by maintaining its functional characteristics and ease of oral delivery transported into different tissues such as muscle and bone after absorption through the intestinal epithelial cells.

IGF-1 is involved in multiple growth signaling pathways including bone growth, fracture healing, and dental tissue regeneration through proliferation and differentiation of chondrogenic and osteogenic cells [11]. For example, IGF-1 enhances osteogenic differentiation of MSCs (Mesenchymal stem cells) towards osteogenic precursor cells, such as osteoblasts [65,66] and also promotes osteogenesis and cementogenesis in periodontal regeneration by boosting proliferation/differentiation of MSCs [67]. Human oral keratinocytes, epidermal stem cells, can be a key source for tooth formation promoting differentiation into enamel-secreting ameloblasts when generated with mouse embryonic

Author Manuscript

mesenchyme [68]. Oral keratinocytes also regulate oral epithelial growth stimulated by keratinocyte growth factors including IGF-1 [69]. The present study demonstrates that chloroplast derived Pro-IGF-1 facilitated proliferation of oral cells including GMSCs (Human Gingiva derived Mesenchymal Stromal Cells), HOK (Human Oral Keratinocytes), and mouse osteoblast with significantly upregulated expression of osteoblast differentiation marker genes. These findings indicate that this study advances the therapeutic capacity of chloroplast derived Pro-IGF-1 for craniofacial and bone treatment. Recent clinical trials have shown that application of recombinant human fibroblast (FGF)-2 and teriparatide (parathyroid 1–34) resulted in bone formation after delivery to periodontal lesion via open flap debridement surgery [70]. Additionally, studies have shown that local administration of IGF-1 in a rat fracture model accelerate fracture healing with stronger callus formation [71,72] and IGF-1 has a similar effect on callus formation when compared to Bone Morphogenetic Protein-2 [73,74]. Moreover, recent clinical trials demonstrated that IGF-1 plays an important role in healing delayed union and high serum levels of IGF-1 correlate with successful treatment outcomes [75–77]. However, despite the promising outcomes, surgery is still required for delivering therapeutic proteins in dental medicine as well as bone healing [70,78]. The chloroplast system offers a platform for a novel periodontal and skeletal drug delivery to increase patient compliance and affordability.

To further examine the effect of orally delivered IGF-1 in an in vivo model, we applied a type I diabetic fracture healing model in this study. Unexpectedly, we did not observe a significant impact on fracture healing after IGF-1 treatment in non-diabetic mice, because endogenous IGF-1 levels were normal. Interestingly, in the pathological diabetic condition, when the bone regeneration is reduced, IGF-1 can restore the defective bone regeneration caused by diabetes. We found that the bone volume, density and area were significantly increased after IGF-1 treatment, when compared to the WT plant treated diabetic mice. It is worth noting that the blood glucose levels are not different between diabetic mice treated with or without IGF-1 during this study. Additionally, IGF-1 sera levels between IGF-1 treated Diabetic and non-Diabetic groups have no significant difference, suggesting diabetes may not affect IGF-1 absorption though GM1 receptor in gut epithelium of mice. Moreover, this also indicated that improved bone formation is due to IGF-1 effect on the bone and not due to improvement of the diabetic condition.

The plant chloroplast system has been advanced to deliver therapeutic proteins with various advantages including a high-level expression and ease of oral administration. However, removal of the antibiotic resistance gene could further improve this process. Previous studies have shown that direct DNA repeats > 600 bp promote homology-based marker excision in tobacco chloroplast genomes [79]. More recently, we have demonstrated the first application of marker-free transplastomic lettuce expressing food/feed enzymes [37,38]. Therefore, to create the Pro-IGF-1, we used 649 bp of two *atpB* promoter regions to initiate the marker excision from the transformed lettuce chloroplast genome. Interestingly, the *aadA* gene was successfully excised even in the first round of selection. This may be due to the copy correction mechanism that maintains identical inverted repeat regions (including spacer regions) found in > 800 sequenced chloroplast genome [80]. These results suggest that generation of marker-free transplastomic edible plants is efficient and precisely removes the selectable marker genes in a short, simple method with no need for additional screening

process. Furthermore, the excision of antibiotic resistance genes not only reduces metabolic load of the transplastomic crops but also enables the same selection marker to be reused for subsequent transformation events.

In conclusion, this study demonstrates that the Pro-IGF-1 expressed in plant chloroplasts and bioencapsulated by the plant cell wall is orally deliverable in fully functional form. Lyophilized plant cells can be stored at room temperature up to 31 months without losing functional efficacy, facilitating affordability and enhanced patient compliance, in sharp contrast to surgical delivery of protein drugs in dental medicine. Precise excision of the antibiotic resistance gene from transformed lettuce chloroplast genome, inclusion of e-peptide to enhance function of IGF-1 not present in current clinical products and ease of repetitive oral drug delivery offer major improvements for patients who suffer from various genetic muscle diseases, acute atrophy, injuries or bone loss.

## 4. Methods

### 4.1. Generation of CTB-Pro-IGF-1 expressing tobacco and lettuce transplastomic lines

To fuse codon-optimized and synthesized Pro-IGF-1 to CTB, overlapping PCR was done using primers which are as follows: *NdeI*-CTB-F, 5' - TTCATATGACACCTCAAATATTACTGATT; CTB-IGF-1, 5' - TTGCCGCAATTAGTATGGCAAATGGTCCTGGACCACGTCGTAAACGCTCTGTTGGT CCTGAAACTCTATGTGGTGCT; IGF-1-*PshAI*-R, 5' - CAATAAGACCAAAGTCTCTAGATTACATACGATAATTTTTGTTTCCAGC; and IGF-1-*XbaI*-R, 5' - CAATAATCTAGATTACATACGATAATTTTTGTTTCCAGC. The resultant CTB-Pro-IGF-1 fusion construct was amplified and cloned into tobacco chloroplast transformation vector (pLD-utr) and lettuce vector (pLsLF) [37,81]. The cloned CTB-Pro-IGF-1 was transformed to tobacco (*Petit Havana*) and Lettuce (*Lactuca sativa*) cv. Simpson Elite by bombardment as previously described [37,81,82]. After the bombardment, shoot regeneration was performed as described previously [80,81]. Primary shoots were screened using PCR with specific primer sets which are as follows: 16s-F, 5' - CAGCAGCCGCGTAATACAGAGGATGCAAGC; aadA-R, 5' - CCGGTTGTTTCATCAAGCCTTACGGTCACC; *NdeI*-CTB-F, 5' - TTCATATGACACCTCAAATATTACTGATT; IGF-1-*PshAI*-R, 5' - CAATAAGACCAAAGTCTCTAGATTACATACGATAATTTTTGTTTCCAGC; UTR-F, 5' - AGGAGCAATAACGCCCTCTTGATAAAAC; and 23s-R, 5' - TGCACCCCTACCTCCTTATCACTGAGC. The PCR positive leaves were subject to the 2nd round selection on regeneration media [81] containing spectinomycin 500 µg/mL for tobacco and 50 µg/mL for lettuce. The regenerated shoots after the 2nd round selection was screened by PCR with the same primer sets used in the 1st round selection. The achievement of homoplasmy and the expression of the fusion proteins in the homoplasmic lines were confirmed using Southern and western blot assay respectively as described below, and the confirmed lines were transferred to hydroponic system and then greenhouse as previously described [37].

#### 4.2. Creation of marker-free PTD-IGF-1 lettuce chloroplast expression vectors

Lettuce chloroplast transformation vector in the Daniell lab, pLsLF, was used as a backbone vector [81], which contains spectinomycin-resistant gene (*aadA*, aminoglycoside 3'-adenylyltransferase gene). To design a marker-removable vector, the 649-bp long direct repeat DNA sequence, derived from *atpB* promoter and 5' UTR [37,38], was PCR amplified using tobacco total genomic DNA as a template and then the sequence-confirmed direct repeats were cloned to flank *aadA* expression cassette. For the insertion of single-digested *atpB* fragments into the vector backbone, NEBuilder HiFi DNA (NEB, Ipswich, MA) assembly kit was used to avoid the possible ligation of the fragments in a reverse direction. The codon-optimized Pro-IGF-1 was also fused to PTD using overlapping PCR and the used primers are as follows: *NdeI*-PTD-F, 5'-ATTTTACATATGAGACACATCAAGATCTGGTTCCAAAACCGCCGCATGAAGTGGAAA; PTD-IGF-1-F, 5'-CCGCCGCATGAAGTGGAAAAAGGGTCCTGGACCACGTCGTAAACGAT; and IGF-1-*PshAI*-R, 5'-CAATAAGACCAAAGTCTCTAGATTACATACGATAATTTTTGTTTCCAGC. The PCR-amplified PTD fused Pro-IGF-1 construct was cloned into the newly designed marker-free vector, pLsLF-MF (please refer to the detailed process of the marker-free vector construction in suppl Fig. 2) and the constructed plasmids were then delivered by gene gun into lettuce (*Lactuca sativa*) cv. Simpson Elite leaves [81].

#### 4.3. Screening of marker-free PTD-Pro-IGF-1

After bombardment, lettuce leaves were cut into small pieces (less than 1 cm<sup>2</sup>) and grown on regeneration media [MS salts (Caisson, Smithfield, UT), Gamborg vitamins (PhytoTechnology Laboratory, Lenexa KS), BAP 0.2 mg (Sigma, St Louis, MO), NAA 0.1 mg (Sigma, St Louis, MO), Myoinositol 100 mg (Sigma, St Louis, MO), PVP 500 mg (Sigma, St Louis, MO), sucrose 30 g (Sigma, St Louis, MO), phytoblend 5 g (PhytoTechnology Laboratory, Lenexa, KS)] containing spectinomycin 50 µg/mL. Primary shoots (4–6 weeks) generated from the selection media were screened using specific PCR primer sets: 16s-F, 5'-CAGCAGCCGCGTAATACAGAGGATGCAAGC; *aadA*-R, 5'-CCGCGTTGTTTCATCAAGCCTTACGGTCACC; *atpB*-R, 5'-GAATTAACCGATCGACGTGCTAGCGGACATT; UTR-F, 5'-AGGAGCAATAACGCCCTCTTGATAAAAC; 23s-R, 5'-TGCACCCCTACCTCCTTTATCACTGAGC. In another round of selection, any regenerated shoots showing bleached leaves were immediately subject to PCR analysis to confirm the excision of *aadA* gene and then transferred to spectinomycin-free media to induce roots. Once the roots were produced, homoplasmy and transgene expression were confirmed by Southern and western blot assay, respectively. For the western blot, fresh leaves were ground in liquid nitrogen; 100 mg of the ground powder was suspended in 300 µL of extraction buffer (100 mM NaCl, 10 mM EDTA, 200 mM Tris-Cl, pH 8, 0.05% v/v Tween 20, 0.1% v/v SDS, 400 mM Sucrose, 14 mM β-mercaptoethanol, 100 mM DTT, 2 mM phenylmethylsulfonyl fluoride, and proteinase inhibitor cocktail). Detailed subsequent steps are described below. Southern blot assay was performed according to manufacturer's protocol of DIG high prime DNA labelling and detection starter kit II (Roche, Penzberg, Germany). The transplastomic plants were grown in AeroGarden hydroponic system for

2 weeks, supplemented with liquid plant food (Miracle-Gro, Marysville, OH), and then transferred to greenhouse for biomass increase. For the growth in the greenhouse, the transplastomic plants were planted in soil, mixed with a 1:1 ratio of garden soil (Miracle-Gro, Marysville, OH) and potting soil (Erthgro), and the plants were fertilized with Miracle-Gro Water Soluble All Purpose Plant Food once or twice per week under the conditions of 16-h: 8-h light cycle at 22 °C. Harvested leaves were lyophilized as previously described [33].

#### 4.4. Quantitation and characterization of CTB/PTD-Pro-IGF-1 in lyophilized cells

To investigate expression of CTB or PTD fused Pro-IGF-1, 10 mg of lyophilized leaf powder was rehydrated in 500  $\mu$ L of extraction buffer (100 mM NaCl, 10 mM EDTA, 200 mM Tris-Cl, pH 8, 0.05% v/v Tween 20, 0.1% v/v SDS, 400 mM Sucrose, 14 mM  $\beta$ -mercaptoethanol, 100 mM DTT, 2 mM phenylmethylsulfonyl fluoride, and proteinase inhibitor cocktail) for 1 h at 4 °C and was then sonicated using Sonicator 3000 (Misonix, Farmingdale, NY) under the conditions of three cycles of 5 s on and 10 s off. After the extracted proteins were quantified by Bradford assay (Bio-rad Laboratories, Hercules, CA), the protein samples were heated at 70 °C in 1X Laemmli sample buffer for 10 min and separated on SDS-PAGE (12%). Immunoprobings were performed using rabbit anti-CTB (1:10,000) (Gen Way Biotech, San Diego, CA), rabbit anti-IGF-1 (1:4,000) (Abcam, Cambridge, UK), and goat anti rabbit IgG-HRP (1:4,000) (Southern Biotechnology, Birmingham, AL). The protein size marker was detected using Precision protein Strep Tactin-HRP conjugate (1:5000) (Bio-rad Laboratories, Hercules, CA). Chemiluminescent signals emitted by HRP were developed onto X-ray films and the developed X-ray films were then analyzed using ImageJ software (IJ 1.46; NIH) for the densitometry assay to quantify the expression levels of the fusion proteins. Standard curves were created using known amounts of CTB protein (Sigma, St Louis, MO) or IGF-1 peptide (Abcam, Cambridge, UK).

#### 4.5. Immunoblots of CTB-Pro-IGF-1 in non-reducing gels

Ten mg of lyophilized tobacco leaf powders was rehydrated in 500  $\mu$ L of the extraction buffer containing no reducing agents such as 14 mM  $\beta$ -mercaptoethanol, 100 mM DTT for 1 h at 4 °C, sonicated, and quantified as described above. After the extracted proteins were mixed with sample buffer (250 mM Tris-Cl, pH 6.5, 10% w/v SDS, 50% v/v glycerol, 0.2 mM bromophenol blue), electrophoresis and western blot were performed as described above.

#### 4.6. Quantitation of Pro-IGF-1 in fresh and lyophilized leaves

Equal amounts of fresh and lyophilized leaf materials were extracted in the same volume of extraction buffer, and the extracted proteins were loaded in a serially diluted way and followed by immunoprobings steps described above. For lettuce lines expressing CTB-Pro-IGF-1 or marker-free PTD-Pro-IGF-1, 1X indicates the volume of 10  $\mu$ L from the resuspended protein samples, which were prepared from the extraction of 10 mg of lyophilized powder in 300  $\mu$ L of protein extraction buffer. The sample preparation of tobacco line expressing CTB-Pro-IGF-1 was the same as the lettuce line but 1X indicates the volume of 1  $\mu$ L. For loading controls, membranes were deprobed using Western Stripping Buffer (Thermo Fisher Scientific, Waltham, MA) for 10 min at 37 °C, then immunolabeled

with rabbit anti-RbcL antibody (Rubisco Large Subunit) (Agrisera, Vannas, Sweden) diluted 1 in 40,000 in PTM for 1 h. The subsequent western blot steps were followed as described above.

#### 4.7. GM1-Ganglioside receptor binding assay

The formation of pentameric structure of CTB-Pro-IGF-1 expressed in both lyophilized tobacco and lettuce was evaluated using CTB-CTB-GM1 binding ELISA. The binding assay was carried out as described previously [6].

#### 4.8. Purification of CTB-Pro-IGF-1 and cell proliferation assay

Four hundred milligrams of lyophilized and ground tobacco transplastomic lines containing CTB-Pro-IGF-1 was rehydrated in 20 mL of plant protein extraction buffer (50 mM NaP, 300 mM NaCl, 1.4 mM beta-mercaptoethanol, 0.5% v/v Tween 20, and 2 tablets of protease inhibitor cocktail, pH 7.8) for 1 h at 4 °C and homogenized. The homogenate was spun down after sonication. The supernatant was incubated with buffer exchanged 2 mL of Ni resin (Clontech, Fremont, CA) for overnight. Once it was stacked up in columns, they were washed in a sequence with 15 mL of binding buffer (50 mM NaP, 300 mM NaCl, pH 7.8) and 30 mL of wash buffer (50 mM NaP, 300 mM NaCl, 20 mM imidazole, pH 7.8). Then, they were eluted with elution buffer (50 mM NaP, 300 mM NaCl, 250 mM imidazole, pH 7.8). Purified CTB-Pro-IGF-1 was evaluated on a Coomassie blue stained gel and its concentration was calculated based on standard curves made with known concentration of IGF-1 peptide (Abcam, Cambridge, UK) on the same protein gel followed by immunoblot analysis as described above. Certain number of cells [2,500 of HOK (Human Oral Keratinocytes), 5,000 of GMSCs (Human Gingiva derived Mesenchymal Stromal Cells), 3,000 of SCCs (Human head and neck Squamous Carcinoma Cells), and 4,000 of MC3TC (Mouse Osteoblast Cells) in 100 µL growth media were seeded in three 96-well plates. After 16 h at 37 °C with 5% CO<sub>2</sub>, a series concentration of the purified CTB-Pro-IGF-1 and human IGF-1 commercial peptide (Abcam, Cambridge, UK) were incubated with the cells. PBS added in the cells was used as negative control for 0 ng of peptide. After 24, 48, and 72 h, absorbance of viable proliferated cells were measured by MTT assay (Roche, Basel, Switzerland) at 570 nm with references at 655 nm. The data was biologically repeated twice run in triplets.

To examine the osteogenic differentiation, MC3T3 cells were treated with osteogenic medium (OS medium). OS medium is  $\alpha$ -MEM (Gibco, Waltham, MA) containing 10% FBS, 10 mM  $\beta$ -glycerophosphate (Sigma, St Louis, MO), 50 µg/ml ascorbic acid (Sigma) and 10<sup>-8</sup> M dexamethasone (Sigma). After 5 days treatment in OS medium with purified CTB-Pro-IGF-1 at 100 ng/ml, 200 ng/ml and 300 ng/ml, cells were isolated for RNA extraction and qPCR analysis for osteogenetic markers: Alkaline phosphatase (ALP), runt related transcription factor 2 (RUNX2) and Osterix (Osx).

#### 4.9. Animal studies

C57BL/6J mice 8–10 weeks of age were purchased from the Jackson Laboratories and housed in pathogen-free conditions at the University of Pennsylvania under institutionally approved protocols. Lyophilized plant cells were rehydrated in PBS to a final volume of 300

$\mu$ L per gavage dose (containing 5  $\mu$ g of CTB or PTD tagged IGF-1) and briefly vortexed for 3–4 s. Three groups of mice, 18 per group (9 males and 9 females) were fed using a 20 gauge gastric gavage needle. Blood (50–80  $\mu$ L) was drawn from the submandibular vein before and 2 h after gavage and allowed to clot at room temperature for 2 h. Subsequently, sera were separated by centrifugation at 3000 RPM for 15 min at 4 °C and stored at –80 °C. Levels of IGF-1 in sera were assessed by ELISA assay. Soleus or gastrocnemius muscles were dissected from the hind limb of controls and mice fed CTB or PTD tagged IGF-1, snap frozen in liquid nitrogen and assessed for IGF-1 by western blot. For kinetic studies, baseline blood was drawn from the sub-mandibular vein of six mice (3 male and 3 female) and subsequently mice were gavaged with plant powder expressing CTB-Pro-IGF-1 as described above. Blood samples were drawn at 2, 6, 8, and 24 h after gavage and sera was collected. IGF-1 levels in sera were determined by ELISA.

#### 4.10. Release of PTD-Pro-IGF-1 from plant cells using cell wall degrading enzymes

Lyophilized lettuce cells expressing PTD-Pro-IGF-1 was incubated in PBS for 5 min and the supernatant was separated by centrifugation (14,000 RPM for 10 min). The pellet was resuspended in PBS in the presence or absence of a mixture of plant cells (5 mg) expressing enzymes (mannanase, pectinate lyase, endoglucanase, exoglucanase). After 2 h incubation at room temperature the supernatant was separated by centrifugation and PTD-IGF-1 was quantitated by ELISA.

#### 4.11. ELISA assay of IGF-1 in sera

IGF-1 standards (Abcam, Cambridge, UK) and sera samples were diluted in coating buffer (15 mM Na<sub>2</sub>CO<sub>3</sub>, 35 mM NaHCO<sub>3</sub>, 3 mM NaH<sub>3</sub>, pH9.6) and allowed to bind to Costar (3590) high-binding EIA/RIA plates overnight. Subsequently, plates were washed 3 times in PBS-0.1% Tween-20 (PBST), blocked with 3% milk in PBST (PTM) for 1 h and incubated in primary antibody, rabbit anti-IGF-1 in PTM 1:2000 (Abcam, Cambridge, UK) for 2 h at 37 °C. Next, plates were washed 3 times in PBST and incubated in secondary antibody goat antirabbit IgG1 conjugated to HRP in PTM 1:4000 (Southern Biotechnology, Birmingham, AL) at 37 °C for 1 h. Plates were then washed in PBST, incubated in TMB peroxidase substrate (Rockland) for 10 min at room temperature, followed by stop solution (2 N H<sub>2</sub>SO<sub>4</sub>). Absorbance was read at 450 nm.

#### 4.12. Immunoblotting analysis of muscle tissues

Soleus and gastrocnemius muscle tissues were thawed from liquid nitrogen and homogenized in lysis buffer (10 vol per muscle wet weight) consisting of 50 mM Tris-HCL, pH 7.4; 0.25% sodium deoxycholate; 150 mM NaCl and 1% Triton X-100; protease and phosphatase inhibitors (Sigma, St Louis, MO). Tissue homogenates were assessed for protein by Bradford assay (Bio-rad Laboratories, Hercules, CA). Tissues were analyzed by electrophoresis and western blotting as described above. For loading controls, the membrane was incubated in Western Stripping Buffer (Thermo Fisher Scientific, Waltham, MA) for 5 min at 37 °C, was incubated in primary antibody mouse anti-actin (Santa Cruz Biotechnology, Dallas TX), 1:4000 or mouse anti-GAPDH (Abcam, Cambridge, UK), 1:4000 in PTM, washed in PBST, and incubated in HRP conjugated goat-anti-mouse IgG (Southern Biotechnology, Birmingham, AL) 1:4000 and developed by chemiluminescence.

#### 4.13. Murine type I diabetic femur fracture model

Twenty-five eight-week old C57BL/6J male mice from Jackson Laboratory were randomly assigned to four groups: CON group (6 male non-diabetic mice, oral gavage with lyophilized wide type (WT) plant cells), IGF-1 group (6 male non-diabetic mice, oral gavage with lyophilized plant cells containing CTB-Pro-IGF-1), Dia group (7 male diabetic mice, oral gavage with lyophilized WT plant cells), Dia-IGF-1 group (6 male diabetic mice, oral gavage with lyophilized plant cells containing CTB-Pro-IGF-1). WT plant cells powder and lyophilized plant cells (20 mg) containing 5 µg CTB-Pro-IGF-1 were respectively rehydrated in PBS to a final volume of 300 µL per gavage dose. The period of oral gavage was 6 weeks and the frequency of it was once a day.

Mice from Dia and Dia-IGF-1 groups were given daily intraperitoneal injections with STZ (50 µg/g body weight in 0.1 M citrate buffer) for 5 days to induce type I diabetes at 3 weeks before fracture as previously described [83]. Blood glucose levels were examined 7 days after the final streptozotocin injection by obtaining blood from tail vein and measuring glucose concentration with a glucometer (ONE TOUCH Ultra 2, LifeScan, Switzerland). Mice with no fasting blood glucose levels greater than 300 mg/dl were considered diabetics.

Closed femoral fractures with intramedullary nail fixation were performed in 12-week (wk)-old mice previously described [84,85]. Briefly, closed fractures were generated by a three-point blunt guillotine driven by a dropped weight, which creates a uniform transverse fracture of the femur. The fractured femurs were harvested at 6 weeks post fracture for analysis.

#### 4.14. Micro-computed tomography (microCT) imaging and radiography

Mice were anesthetized by isoflurane and the fracture sites were radiographed using a Faxitron MX-20 (Faxitron X-Ray) at D0, D7, D14 and D21 to monitor the progress of fracture healing. At the end of this study, bone microarchitecture of the fractured femur was tested using Scanco Medical µCT 35 at the Imaging Core, Penn Center for Musculoskeletal Disorders. Scans were performed at 55 keV and 3D images were reconstructed at the fracture line extending at least 3 mm to the proximal and distal. The ratio of the bone volume to the total volume (BV/TV) and bone density were determined in the fracture callus with density thresholds set at 300 mg/cm<sup>3</sup> HA.

#### 4.15. Histological analyses

Fracture calluses were excised, fixed with 4% paraformaldehyde and decalcified in 10% ethylenediaminetetraacetic acid (EDTA) for a minimum three weeks at 4°C. The samples were then embedded in OCT. Longitudinal sections (8 µm thick) were cut from the mid-portion of the callus and mounted serially on gelatin-coated glass slides and stained with hematoxylin and eosin (Sigma-Aldrich) for histological examination. The morphological characteristics of bone healing were observed by Leica fluorescent microscope (DMI6000B, Leica, Germany).

## Supplementary Material

Refer to Web version on PubMed Central for supplementary material.

## Acknowledgements

Authors thank Profs. Barton (University of Florida) and Day (University of Manchester) for critical discussions and Drs. Graves, Hajishengallis, and Le for providing HOK, Osteoblasts, and GMSC/SCC cells.

### Funding

This study was supported by NIH Grants R01 GM 63879, R01 HL 107904, R01 HL 109442, R01 HL 133191 grants to Henry Daniell, and R01 DE023105, R01 AR066101 to Shuying Yang.

## References

- [1]. Sandow J, Landgraf W, Becker R, Seipke G, Equivalent recombinant human insulin preparations and their place in therapy, *Eur. Endocrinol* 11 (2015) 10–16. [PubMed: 29632560]
- [2]. Daniell H, Chan HT, Pasoreck EK, Vaccination via chloroplast genetics: affordable protein drugs for the prevention and treatment of inherited or infectious human diseases, *Annu. Rev. Genet* 50 (2016) 595–618. [PubMed: 27893966]
- [3]. Shaaltiel Y, Gingis-Velitski S, Tzaban S, Fiks N, Tekoah Y, Aviezer D, Plant-based oral delivery of beta-glucocerebrosidase as an enzyme replacement therapy for Gaucher's disease, *Plant Biotechnol. J* 13 (2015) 1033–1040. [PubMed: 25828481]
- [4]. Xu J, Zhang N, On the way to commercializing plant cell culture platform for biopharmaceuticals: present status and prospect, *Pharm. Bioprocess* 2 (2014) 499–518. [PubMed: 25621170]
- [5]. Taliglucerase (Elelyso) for Gaucher Disease, *Med. Lett. Drugs Ther* 54 (2012) 56–56.
- [6]. Su J, Zhu LQ, Sherman A, Wang XM, Lin SN, Kamesh A, Norikane JH, Streatfield SJ, Herzog RW, Daniell H, Low cost industrial production of coagulation factor IX bioencapsulated in lettuce cells for oral tolerance induction in hemophilia B, *Biomaterials* 70 (2015) 84–93. [PubMed: 26302233]
- [7]. Herzog RW, Nichols TC, Su J, Zhang B, Sherman A, Merricks EP, Raymer R, Perrin GQ, Hager M, Wiinberg B, Daniell H, Oral tolerance induction in hemophilia B dogs fed with transplastomic lettuce, *Mol. Ther* 25 (2017) 512–522. [PubMed: 28153098]
- [8]. Kwon KC, Daniell H, Oral delivery of protein drugs bioencapsulated in plant cells, *Mol. Ther* 24 (2016) 1342–1350. [PubMed: 27378236]
- [9]. Daniell H, Kulis M, Herzog RW, Plant cell-made protein antigens for induction of Oral tolerance, *Biotechnol. Adv* (2019).
- [10]. Tilles SA, Petroni D, FDA-approved peanut allergy treatment the first wave is about to crest, *Ann. Allergy Asthma Immunol* 121 (2018) 145–149. [PubMed: 29909055]
- [11]. Bikle DD, Tahimic C, Chang WH, Wang YM, Philippou A, Barton ER, Role of IGF-I signaling in muscle bone interactions, *Bone* 80 (2015) 79–88. [PubMed: 26453498]
- [12]. Heatwole CR, Eichinger KJ, Friedman DI, Hilbert JE, Jackson CE, Logigian EL, Martens WB, McDermott MP, Pandya SK, Quinn C, Smirnow AM, Thornton CA, Moxley RT 3rd, Open-label trial of recombinant human insulin-like growth factor 1/recombinant human insulin-like growth factor binding protein 3 in myotonic dystrophy type 1, *Arch. Neurol* 68 (2011) 37–44. [PubMed: 20837825]
- [13]. Govoni KE, Wergedal JE, Florin L, Angel P, Baylink DJ, Mohan S, Conditional deletion of insulin-like growth factor-I in collagen type 1 alpha 2-expressing cells results in postnatal lethality and a dramatic reduction in bone accretion, *Endocrinology* 148 (2007) 5706–5715. [PubMed: 17717052]
- [14]. Jiang J, Lichtler AC, Gronowicz GA, Adams DJ, Clark SH, Rosen CJ, Kream BE, Transgenic mice with osteoblast-targeted insulin-like growth factor-I show increased bone remodeling, *Bone* 39 (2006) 494–504. [PubMed: 16644298]

- [15]. Kanazawa I, Yamaguchi T, Yamamoto M, Yamauchi M, Yano S, Sugimoto T, Serum insulin-like growth factor-I level is associated with the presence of vertebral fractures in postmenopausal women with type 2 diabetes mellitus, Osteoporos. Int 18 (2007) 1675–81. [PubMed: 17632742]
- [16]. Sugimoto T, Nishiyama K, Kuribayashi F, Chihara K, Serum levels of insulin-like growth factor (IGF) I, IGF-binding protein (IGFBP)-2, and IGFBP-3 in osteoporotic patients with and without spinal fractures, J. Bone Miner. Res 12 (1997) 1272–1279. [PubMed: 9258758]
- [17]. Schmidmaier G, Wildemann B, Heeger J, Gabelein T, Flyvbjerg A, Bail HJ, Raschke M, Improvement of fracture healing by systemic administration of growth hormone and local application of insulin-like growth factor-1 and transforming growth factor-beta1, Bone 31 (2002) 165–72. [PubMed: 12110430]
- [18]. Locatelli V, Bianchi VE, Effect of GH/IGF-1 on bone metabolism and osteoporosis, Internet J. Endocrinol 2014 (2014) 235060.
- [19]. Chen QQ, Wang WM, Expression of FGF-2 and IGF-1 in diabetic rats with fracture, Asian Pac. J. Trop. Med 7 (2014) 71–75. [PubMed: 24418087]
- [20]. Tahimic CG, Wang Y, Bikle DD, Anabolic effects of IGF-1 signaling on the skeleton, Front Endocrinol. (Lausanne) 4 (2013) 6. [PubMed: 23382729]
- [21]. Wang S, Mu J, Fan Z, Yu Y, Yan M, Lei G, Tang C, Wang Z, Zheng Y, Yu J, Zhang G, Insulin-like growth factor 1 can promote the osteogenic differentiation and osteogenesis of stem cells from apical papilla, Stem Cell Res 8 (2012) 346–356. [PubMed: 22286010]
- [22]. Philippou A, Maridaki M, Pneumaticos S, Koutsilieris M, The complexity of the IGF1 gene splicing, posttranslational modification and bioactivity, Mol. Med 20 (2014) 202–214. [PubMed: 24637928]
- [23]. Durzynska J, Philippou A, Brisson BK, Nguyen-McCarty M, Barton ER, The proforms of insulin-like growth factor I (IGF-I) are predominant in skeletal muscle and alter IGF-I receptor activation, Endocrinology 154 (2013) 1215–1224. [PubMed: 23407451]
- [24]. Philippou A, Barton ER, Optimizing IGF-I for skeletal muscle therapeutics, Growth Hormone IGF Res 24 (2014) 157–163.
- [25]. Barton ER, DeMeo J, Lei HQ, The insulin-like growth factor (IGF)-I E-peptides are required for isoform-specific gene expression and muscle hypertrophy after local IGF-I production, J. Appl. Physiol 108 (2010) 1069–1076. [PubMed: 20133429]
- [26]. Bally J, Nadai M, Vitel M, Rolland A, Dumain R, Dubald M, Plant physiological adaptations to the massive foreign protein synthesis occurring in recombinant chloroplasts, Plant Physiol 150 (2009) 1474–1481. [PubMed: 19458113]
- [27]. Zhang B, Shanmugaraj B, Daniell H, Expression and functional evaluation of biopharmaceuticals made in plant chloroplasts, Curr. Opin. Chem. Biol 38 (2017) 17–23. [PubMed: 28229907]
- [28]. Sanz-Barrio R, Millan AF, Corral-Martinez P, Segui-Simarro JM, Farran I, Tobacco plastidial thioredoxins as modulators of recombinant protein production in transgenic chloroplasts, Plant Biotechnol. J 9 (2011) 639–650. [PubMed: 21426478]
- [29]. Xie TT, Qiu QC, Zhang W, Ning TT, Yang W, Zheng CY, Wang C, Zhu YG, Yang DC, A biologically active rhIGF-1 fusion accumulated in transgenic rice seeds can reduce blood glucose in diabetic mice via oral delivery, Peptides 29 (2008) 1862–1870. [PubMed: 18708105]
- [30]. Daniell H, Ruiz G, Denes B, Sandberg L, Langridge W, Optimization of codon composition and regulatory elements for expression of human insulin like growth factor-1 in transgenic chloroplasts and evaluation of structural identity and function, BMC Biotechnol 9 (2009) 33. [PubMed: 19344517]
- [31]. Poudel SB, Bhattarai G, Kook SH, Shin YJ, Kwon TH, Lee SY, Lee JC, Recombinant human IGF-1 produced by transgenic plant cell suspension culture enhances new bone formation in calvarial defects, Growth Hormone IGF Res 36 (2017) 1–10.
- [32]. Queiroz LN, Maldaner FR, Mendes EA, Sousa AR, D'Allastta RC, Mendonca G, Mendonca DBS, Aragao FJL, Evaluation of lettuce chloroplast and soybean cotyledon as platforms for production of functional bone morphogenetic protein 2, Transgenic Res 28 (2019) 213–224. [PubMed: 30888592]

- [33]. Kwon KC, Chan HT, Leon IR, Williams-Carrier R, Barkan A, Daniell H, Codon optimization to enhance expression yields insights into chloroplast translation, *Plant Physiol* 172 (2016) 62–77. [PubMed: 27465114]
- [34]. Duguay SJ, Jie LZ, Steiner DF, Mutational analysis of the Insulin-like Growth-Factor-I prohormone processing site, *J. Biol. Chem* 270 (1995) 17566–17574. [PubMed: 7615562]
- [35]. Limaye A, Koya V, Samsam M, Daniell H, Receptor-mediated oral delivery of a bioencapsulated green fluorescent protein expressed in transgenic chloroplasts into the mouse circulatory system, *FASEB J* 20 (2006) 959–961. [PubMed: 16603603]
- [36]. Sanchez J, Holmgren J, Cholera toxin structure, gene regulation and pathophysiological and immunological aspects, *Cell. Mol. Life Sci* 65 (2008) 1347–1360. [PubMed: 18278577]
- [37]. Daniell H, Ribeiro T, Lin S, Saha P, McMichael C, Chowdhary R, Agarwal A, Validation of leaf and microbial pectinases: commercial launching of a new platform technology, *Plant Biotechnol. J* 17 (2019) 1154–1166. [PubMed: 30963657]
- [38]. Kumari U, Singh R, Ray T, Rana S, Saha P, Malhotra K, Daniell H, Validation of leaf enzymes in the detergent and textile industries: launching of a new platform technology, *Plant Biotechnol. J* 17 (2019) 1167–1182. [PubMed: 30963679]
- [39]. Burrin DG, Wester TJ, Davis TA, Amick S, Heath JP, Orally administered IGF-I increases intestinal mucosal growth in formula-fed neonatal pigs, *Am. J. Physiol. Regul. Integr. Comp. Physiol* 270 (1996) R1085–R1091.
- [40]. Fouque D, Peng SC, Shamir E, Kopple JD, Recombinant human insulin-like growth factor-1 induces an anabolic response in malnourished CAPD patients, *Kidney Int* 57 (2000) 646–654. [PubMed: 10652043]
- [41]. Xiao YH, Kwon KC, Hoffman BE, Kamesh A, Jones NT, Herzog RW, Daniell H, Low cost delivery of proteins bioencapsulated in plant cells to human non-immune or immune modulatory cells, *Biomaterials* 80 (2016) 68–79. [PubMed: 26706477]
- [42]. Flint HJ, Bayer EA, Rincon MT, Lamed R, White BA, Polysaccharide utilization by gut bacteria: potential for new insights from genomic analysis, *Nat. Rev. Microbiol* 6 (2008) 121–131. [PubMed: 18180751]
- [43]. Shenoy V, Kwon KC, Rathinasabapathy A, Lin SN, Jin GY, Song CJ, Shil P, Nair A, Qi YF, Li QH, Francis J, Katovich MJ, Daniell H, Raizada MK, Oral delivery of angiotensin-converting enzyme 2 and angiotensin-(1-7) bioencapsulated in plant cells attenuates pulmonary hypertension, *Hypertension* 64 (2014) 1248–U202. [PubMed: 25225206]
- [44]. Shil PK, Kwon KC, Zhu P, Verma A, Daniell H, Li Q, Oral delivery of ACE2/Ang-(1-7) bioencapsulated in plant cells protects against experimental uveitis and autoimmune uveoretinitis, *Mol. Ther* 22 (2014) 2069–2082. [PubMed: 25228068]
- [45]. Kwon KC, Nityanandam R, New JS, Daniell H, Oral delivery of bioencapsulated exendin-4 expressed in chloroplasts lowers blood glucose level in mice and stimulates insulin secretion in beta-TC6 cells, *Plant Biotechnol. J* 11 (2013) 77–86. [PubMed: 23078126]
- [46]. Boyhan D, Daniell H, Low-cost production of proinsulin in tobacco and lettuce chloroplasts for injectable or oral delivery of functional insulin and C-peptide, *Plant Biotechnol. J* 9 (2011) 585–598. [PubMed: 21143365]
- [47]. Kwon KC, Sherman A, Chang WJ, Kamesh A, Biswas M, Herzog RW, Daniell H, Expression and assembly of largest foreign protein in chloroplasts: oral delivery of human FVIII made in lettuce chloroplasts robustly suppresses inhibitor formation in haemophilia A mice, *Plant Biotechnol. J* 16 (2017) 1148–1160. [PubMed: 29106782]
- [48]. Sherman A, Su J, Lin S, Wang X, Herzog RW, Daniell H, Suppression of inhibitor formation against FVIII in a murine model of hemophilia A by oral delivery of antigens bioencapsulated in plant cells, *Blood* 124 (2014) 1659–1668. [PubMed: 24825864]
- [49]. Su J, Sherman A, Doerfler PA, Byrne BJ, Herzog RW, Daniell H, Oral delivery of Acid Alpha Glucosidase epitopes expressed in plant chloroplasts suppresses antibody formation in treatment of Pompe mice, *Plant Biotechnol. J* 13 (2015) 1023–1032. [PubMed: 26053072]
- [50]. Wang X, Su J, Sherman A, Rogers GL, Liao G, Hoffman BE, Leong KW, Terhorst C, Daniell H, Herzog RW, Plant-based oral tolerance to hemophilia therapy employs a complex immune

- regulatory response including LAP+CD4+ T cells, *Blood* 125 (2015) 2418–2427. [PubMed: 25700434]
- [51]. Arlen PA, Singleton M, Adamovicz JJ, Ding Y, Davoodi-Semiromi A, Daniell H, Effective plague vaccination via oral delivery of plant cells expressing F1-V antigens in chloroplasts, *Infect. Immun* 76 (2008) 3640–3650. [PubMed: 18505806]
- [52]. Chan HT, Xiao Y, Weldon WC, Oberste SM, Chumakov K, Daniell H, Cold chain and virus-free chloroplast-made booster vaccine to confer immunity against different poliovirus serotypes, *Plant Biotechnol. J* 14 (2016) 2190–2200. [PubMed: 27155248]
- [53]. Daniell H, Lee SB, Panchal T, Wiebe PO, Expression of the native cholera toxin B subunit gene and assembly as functional oligomers in transgenic tobacco chloroplasts, *J. Mol. Biol* 311 (2001) 1001–1009. [PubMed: 11531335]
- [54]. Daniell H, Rai V, Xiao Y, Cold chain and virus-free oral polio booster vaccine made in lettuce chloroplasts confers protection against all three poliovirus serotypes, *Plant Biotechnol. J* 17 (2019) 1357–1368. [PubMed: 30575284]
- [55]. Davoodi-Semiromi A, Schreiber M, Nalapalli S, Verma D, Singh ND, Banks RK, Chakrabarti D, Daniell H, Chloroplast-derived vaccine antigens confer dual immunity against cholera and malaria by oral or injectable delivery, *Plant Biotechnol. J* 8 (2010) 223–242. [PubMed: 20051036]
- [56]. Kanagaraj AP, Verma D, Daniell H, Expression of dengue-3 pre-membrane and envelope polyprotein in lettuce chloroplasts, *Plant Mol. Biol* 76 (2011) 323–333. [PubMed: 21431782]
- [57]. Koya V, Moayeri M, Leppla SH, Daniell H, Plant-based vaccine: mice immunized with chloroplast-derived anthrax protective antigen survive anthrax lethal toxin challenge, *Infect. Immun* 73 (2005) 8266–8274. [PubMed: 16299323]
- [58]. Lakshmi PS, Verma D, Yang X, Lloyd B, Daniell H, Low cost tuberculosis vaccine antigens in capsules: expression in chloroplasts, bio-encapsulation, stability and functional evaluation in vitro, *PLoS One* 8 (2013) e54708. [PubMed: 23355891]
- [59]. Watson J, Koya V, Leppla SH, Daniell H, Expression of *Bacillus anthracis* protective antigen in transgenic chloroplasts of tobacco, a non-food/feed crop, *Vaccine* 22 (31–32) (2004) 4374–4384. [PubMed: 15474731]
- [60]. Xiao Y, Daniell H, Long-term evaluation of mucosal and systemic immunity and protection conferred by different polio booster vaccines, *Vaccine* 35 (2017) 5418–5425. [PubMed: 28111147]
- [61]. Holmgren J, Lonnroth I, Mansson J, Svennerholm L, Interaction of cholera toxin and membrane GM1 ganglioside of small intestine, *Proc. Natl. Acad. Sci. U. S. A* 72(7) (1975) 2520–2524. [PubMed: 1058471]
- [62]. Helander HF, Fandriks L, Surface area of the digestive tract - revisited, *Scand. J. Gastroenterol* 49 (2014) 681–689. [PubMed: 24694282]
- [63]. Ruhlman T, Ahangari R, Devine A, Samsam M, Daniell H, Expression of cholera toxin B-proinsulin fusion protein in lettuce and tobacco chloroplasts - oral administration protects against development of insulinitis in non-obese diabetic mice, *Plant Biotechnol. J* 5 (2007) 495–510. [PubMed: 17490448]
- [64]. Hinson J, Raven RP, Chew S, *The Hypothalamus and Pituitary part II: the Anterior Pituitary, the Endocrine System*, second ed., Churchill Livingstone, Edinburgh, 2010, pp. 39–51.
- [65]. Granero-Molto F, Myers TJ, Weis JA, Longobardi L, Li T, Yan Y, Case N, Rubin J, Spagnoli A, Mesenchymal stem cells expressing insulin-like growth factor-I (MSCIGF) promote fracture healing and restore new bone formation in *Irs1* knockout mice: analyses of MSCIGF autocrine and paracrine regenerative effects, *Stem Cells* 29 (2011) 1537–1548. [PubMed: 21786367]
- [66]. Myers TJ, Yan Y, Granero-Molto F, Weis JA, Longobardi L, Li T, Li Y, Contaldo C, Ozkhan H, Spagnoli A, Systemically delivered insulin-like growth factor-I enhances mesenchymal stem cell-dependent fracture healing, *Growth Factors* 30 (2012) 230–241. [PubMed: 22559791]
- [67]. Hernandez-Monjaraz B, Santiago-Osorio E, Monroy-Garcia A, Ledesma-Martinez E, Mendoza-Nunez VM, Mesenchymal stem cells of dental origin for inducing tissue regeneration in periodontitis: a mini-review, *Int. J. Mol. Sci* 19 (2018).

- [68]. Wang B, Li L, Du S, Liu C, Hu X, Chen Y, Zhang Y, O24-induction of human keratinocytes into enamel -secreting ameloblasts, *Bull. Groupement Int. Rech. Sci. Stomatol. Odontol* 49 (2011) 89–89.
- [69]. Costea DE, Loro LL, Dimba EAO, Vintermyr OK, Johannessen AC, Crucial effects of fibroblasts and keratinocyte growth factor on morphogenesis of reconstituted human oral epithelium, *J. Investig. Dermatol* 121 (2003) 1479–1486. [PubMed: 14675199]
- [70]. Rios HF, Bashutski JD, McAllister BS, Murakami S, Cobb CM, Chun YHP, Lin Z, Mandelaris GA, Cochran DL, Emerging regenerative approaches for periodontal reconstruction: practical applications from the AAP regeneration workshop, *Clin. Adv. Periodontics* 5 (2015) 40–46. [PubMed: 26146593]
- [71]. Schmidmaier G, Wildemann B, Heeger J, Gabelein T, Flyvbjerg A, Bail HJ, Raschke M, Improvement of fracture healing by systemic administration of growth hormone and local application of insulin-like growth factor-1 and transforming growth factor-beta 1, *Bone* 31 (2002) 165–172. [PubMed: 12110430]
- [72]. Schmidmaier G, Wildemann B, Bail H, Lucke M, Fuchs T, Stemberger A, Flyvbjerg A, Haas NP, Raschke M, Local application of growth factors (insulin-like growth factor-1 and transforming growth factor-beta 1) from a biodegradable poly(D,L-lactide) coating of osteosynthetic implants accelerates fracture healing in rats, *Bone* 28 (2001) 341–350. [PubMed: 11336914]
- [73]. Schmidmaier G, Lucke M, Schwabe P, Raschke M, Haas NP, Wildemann B, Collective review: bioactive implants coated with poly(D,L-lactide) and growth factors IGF-I, TGF-beta1, or BMP-2 for stimulation of fracture healing, *J. Long Term Eff. Med. Implant* 16 (2006) 61–69.
- [74]. Wildemann B, Burkhardt N, Luebberstedt M, Vordemvenne T, Schmidmaier G, Proliferating and differentiating effects of three different growth factors on pluripotent mesenchymal cells and osteoblast like cells, *J. Orthop. Surg. Res* 2 (2007) 27–27. [PubMed: 18093345]
- [75]. Westhauser F, Zimmermann G, Moghaddam S, Bruckner T, Schmidmaier G, Biglari B, Moghaddam A, Reaming in treatment of non-unions in long bones: cytokine expression course as a tool for evaluation of non-union therapy, *Arch. Orthop. Trauma Surg* 135 (2015) 1107–1116. [PubMed: 26085339]
- [76]. Fischer C, Doll J, Tanner M, Bruckner T, Zimmermann G, Helbig L, Biglari B, Schmidmaier G, Moghaddam A, Quantification of TGF-beta 1, PDGF and IGF-1 cytokine expression after fracture treatment vs. non-union therapy via masquetelet, *Inj. Int. J. Care Inj* 47 (2016) 342–349.
- [77]. Weiss S, Henle P, Bidlingmaier M, Moghaddam A, Kasten P, Zimmermann G, Systemic response of the GH/IGF-I axis in timely versus delayed fracture healing, *Growth Hormone IGF Res* 18 (2008) 205–212.
- [78]. Richardson CR, Allen EP, Chambrone L, Langer B, McGuire MK, Zabalegui I, Zadeh HH, Tatakis DN, Periodontal soft tissue root coverage procedures: practical applications from the AAP regeneration workshop (vol 5, pg 2, 2015), *Clin. Adv. Periodontics* 5 (2015) 151–151. [PubMed: 32781811]
- [79]. Iamtham S, Day A, Removal of antibiotic resistance genes from transgenic tobacco plastids, *Nat. Biotechnol* 18 (2000) 1172–1176. [PubMed: 11062436]
- [80]. Daniell H, Lin CS, Yu M, Chang WJ, Chloroplast genomes: diversity, evolution, and applications in genetic engineering, *Genome Biol* 17 (2016) 134. [PubMed: 27339192]
- [81]. Verma D, Samson NP, Koya V, Daniell H, A protocol for expression of foreign genes in chloroplasts, *Nat. Protoc* 3 (2008) 739–758. [PubMed: 18388956]
- [82]. Ruhlman T, Verma D, Samson N, Daniell H, The role of heterologous chloroplast sequence elements in transgene integration and expression, *Plant Physiol* 152 (2010) 2088–2104. [PubMed: 20130101]
- [83]. Alblowi J, Tian C, Siqueira MF, Kayal RA, McKenzie E, Behl Y, Gerstenfeld L, Einhorn TA, Graves DT, Chemokine expression is upregulated in chondrocytes in diabetic fracture healing, *Bone* 53 (2013) 294–300. [PubMed: 23262028]
- [84]. Kayal RA, Tsatsas D, Bauer MA, Allen B, Al-Sebaei MO, Kakar S, Leone CW, Morgan EF, Gerstenfeld LC, Einhorn TA, Graves DT, Diminished bone formation during diabetic fracture healing is related to the premature resorption of cartilage associated with increased osteoclast activity, *J. Bone Miner. Res* 22 (2007) 560–568. [PubMed: 17243865]

- [85]. Lim JC, Ko KI, Mattos M, Fang M, Zhang C, Feinberg D, Sindi H, Li S, Alblowi J, Kayal RA, Einhorn TA, Gerstenfeld LC, Graves DT, TNFalpha contributes to diabetes impaired angiogenesis in fracture healing, *Bone* 99 (2017) 26–38. [PubMed: 28285015]

Author Manuscript

Author Manuscript

Author Manuscript

Author Manuscript

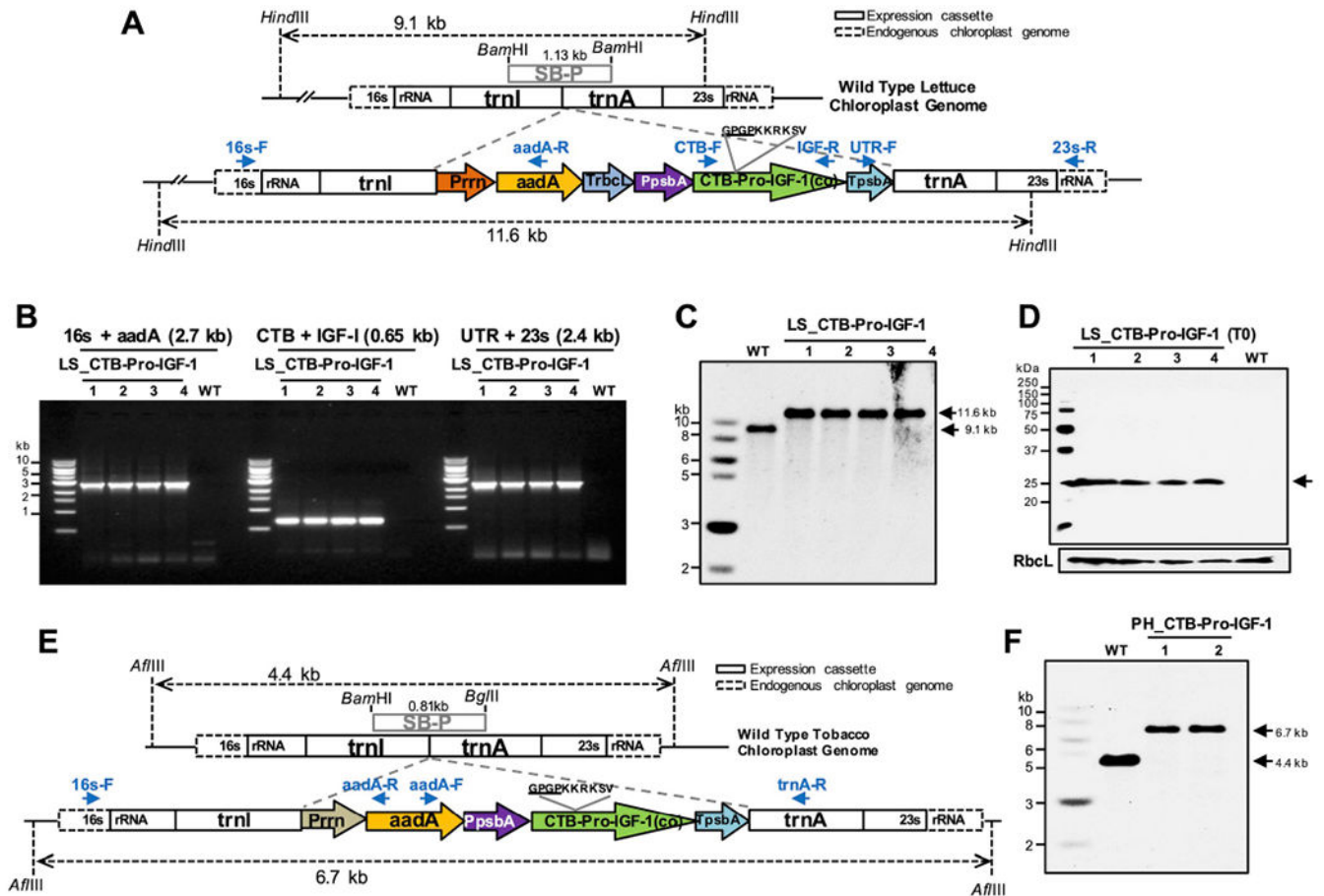


**Fig. 1. Generation of lettuce/tobacco transplastomic lines expressing codon-optimized CTB-Pro-IGF-1 gene.**

(A) Schematic illustration of CTB-Pro-IGF-1 expression cassette for lettuce chloroplast transformation. (A and E) 16s rRNA and 23s rRNA, 16s and 23s ribosomal RNA; *trnI*, isoleucyl-tRNA; *trnA*, alanyl-tRNA; Prmn, rRNA operon promoter; *aadA*, aminoglycoside 3'-adenylyltransferase; *TrbcL*, 3' UTR of ribulose biphosphate carboxylase large subunit; *PpsbA*, promoter of *psbA*; CTB-Pro-IGF-1(co), codon optimized premature form of human insulin-like growth factor-1 with CTB (Cholera non-toxic B subunit) fusion; *TpsbA*, 3'-UTR of *psbA*; SB-P, Southern blot probe. Primer sets used for PCR screening are indicated in arrows. (B) Genomic DNA PCR screening, (C) Southern blot analysis, and (D) Protein expressions of the lettuce lines expressing CTB-Pro-IGF-1. Expected sizes are indicated in arrows (24.3 kDa). (B-D) Lanes 1 to 4, individual transplastomic lines; WT, untransformed wild type; LS, lettuce. (E) Schematic illustration of CTB-Pro-IGF-1 expression cassette for tobacco chloroplast transformation. (F) Southern blot analysis of CTB-Pro-IGF1 tobacco transplastomic lines. WT, untransformed wild type; lanes 1 and 2, transplastomic lines; PH, tobacco Petit Havana.

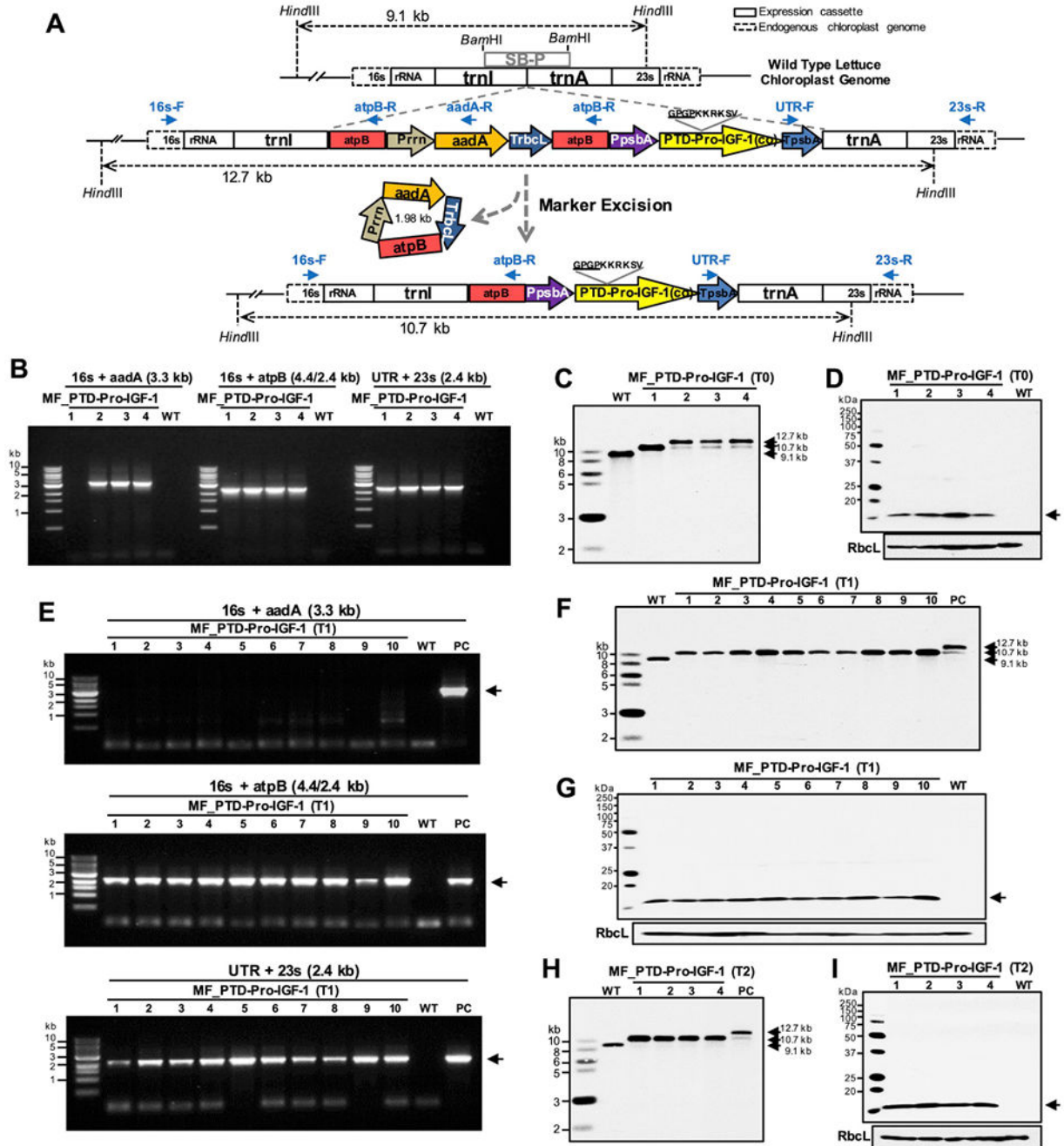


**Fig. 2. Generation of marker-free lettuce transplastomic lines expressing codon-optimized PTD-Pro-IGF-1 gene.**

(A) Schematic diagram of chloroplast transformation vector containing PTD-Pro-IGF-1 expression cassette and marker excision process. 16s rRNA and 23s rRNA, 16s and 23s ribosomal RNA; trnI, isoleucyl-tRNA; atpB, chloroplast encoded CF1 ATP synthase subunit beta; Prn, rRNA operon promoter; aadA, aminoglycoside 3'-adenylyltransferase; TrbcL, 3' UTR of ribulose biphosphate carboxylase large subunit; PpsbA, promoter of psbA; PTD-Pro-IGF-1(co), PTD (Protein Transduction Domains) fused codon optimized premature form of human insulin-like growth factor-1; TpsbA, 3'-UTR of psbA; trnA, alanyl-tRNA; SB-P,

Southern blot probe. **(B)** Genomic DNA PCR screening, **(C)** Southern blot, and **(D)** Protein expression of PTD-Pro-IGF-1 lines. Expected size is indicated in an arrow (14.5 kDa). **(B–D)** Lanes 1 to 4, four individual T0 transplastomic lines; WT, untransformed wild type; MF, lettuce marker-free. **(E)** PCR screening **(F)** Southern blot, and **(G)** Protein expression of PTD-Pro-IGF-1 in antibiotic-free T1 generation. **(E and F)** Lanes 1 to 10; ten individual T1 transplastomic plants, WT; untransformed wild type lettuce; PC, positive control with marker. Expected sizes are indicated in arrows (3.3/2.4/2.4 kb of PCR products and 14.5 kDa of PTD-Pro-IGF-1). **(H)** Southern blot and **(I)** protein expression of PTD-Pro-IGF-1 in antibiotic-free T2 generation. **(H and I)** Lanes 1 to 4; four individual T2 transplastomic plants, WT; untransformed wild type lettuce. Expected sizes are indicated in arrows (14.5 kDa).

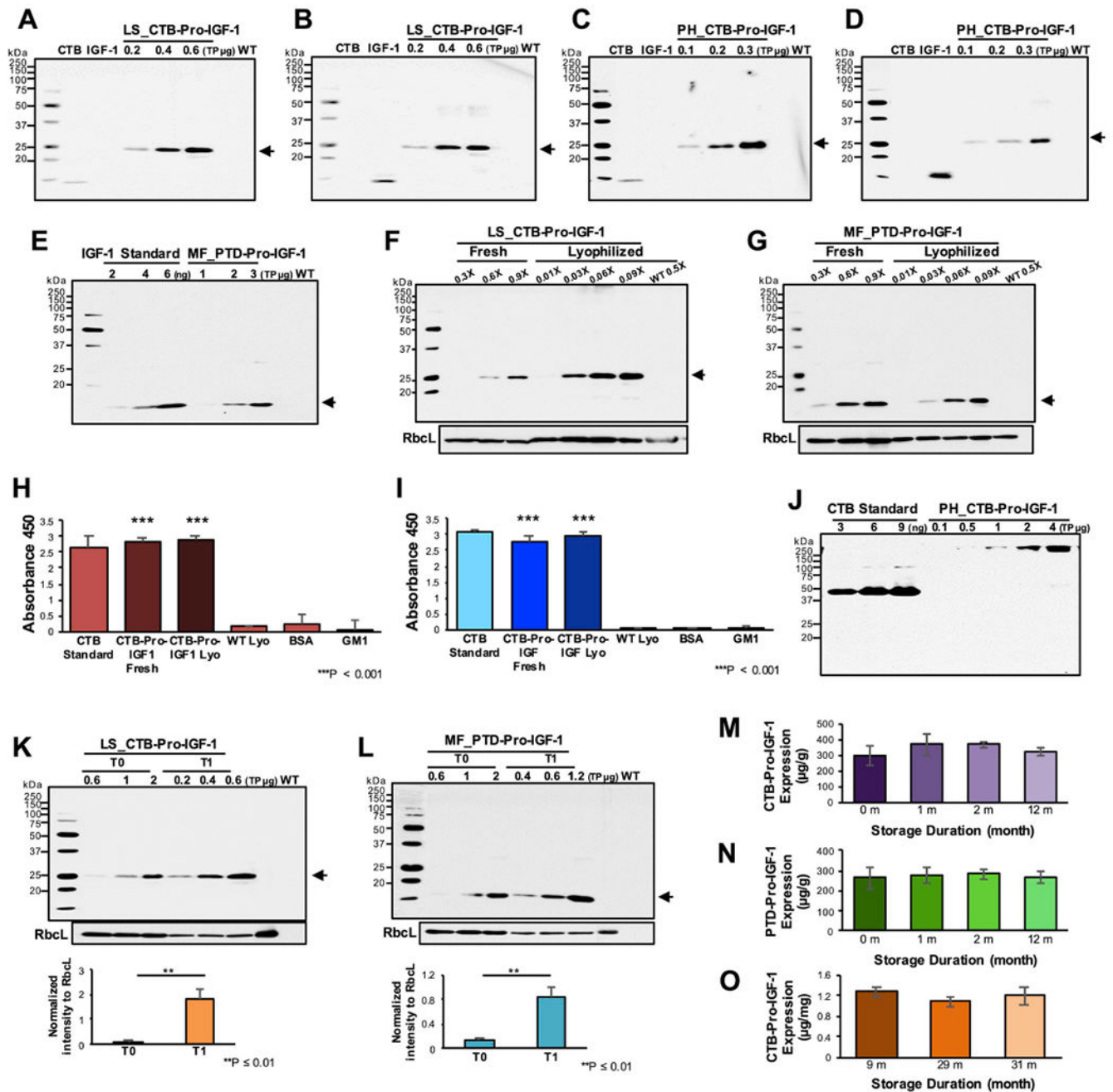


**Fig. 3. Characterizations of CTB/PTD-Pro-IGF-1 in lettuce/tobacco transplastomic lines.** (A–D) Immunoblot assays of CTB-Pro-IGF-1 expressed in (A and B) lettuce and (C and D) tobacco lyophilized cells against (A and C) anti-CTB and (B and D) anti-IGF-1. (E) Quantification of PTD-Pro-IGF-1 expressed in marker-free lettuce lyophilized cells. (F and G) Comparison of CTB/PTD-Pro-IGF-1 expressions in between equal amount (1X) of fresh and lyophilized leaf materials. (F) Lettuce CTB-Pro-IGF-1 and (G) marker-free lettuce PTD-Pro-IGF-1 transplastomic lines. RbcL was used as loading controls. (A–G, K and L) Approximately 24.3 kDa of CTB-Pro-IGF-1 protein and 14.5 kDa of PTD-Pro-IGF-1 are

indicated in arrows. PH, tobacco Petit Havana; LS, lettuce; MF, marker-free lettuce; WT, untransformed wild type tobacco or lettuce. CTB or IGF-1 peptide were used as controls. **(H and I)** ELISA of CTB-Pro-IGF-1 pentamer form in **(H)** lettuce and **(I)** tobacco binding to GM1 receptor. The data is representative of two biological repeats run in triplets. Data are expressed as the mean  $\pm$  SEM (\*\*P-value < 0.001 vs. wild type by ANOVA). CTB was used as positive controls. Lyo, lyophilized leaves. **(J)** Non-reducing immunoblot analysis of tobacco CTB-Pro-IGF-1 against anti-CTB. **(K and L)** Comparison of **(K)** CTB-Pro-IGF-1 and **(L)** PTD-Pro-IGF-1 expressions in between T0 and T1 generations. RbcL was used as loading controls. Data are expressed as the mean  $\pm$  SEM (\*\*P-value = 0.01 by ANOVA). **(M–O)** Stability of **(M)** lettuce CTB-Pro-IGF-1, **(N)** lettuce PTD-Pro-IGF-1 or **(O)** tobacco CTB-Pro-IGF-1 during long-term storage. Data are shown as the mean  $\pm$  SD (P-value > 0.5 by ANOVA between groups).

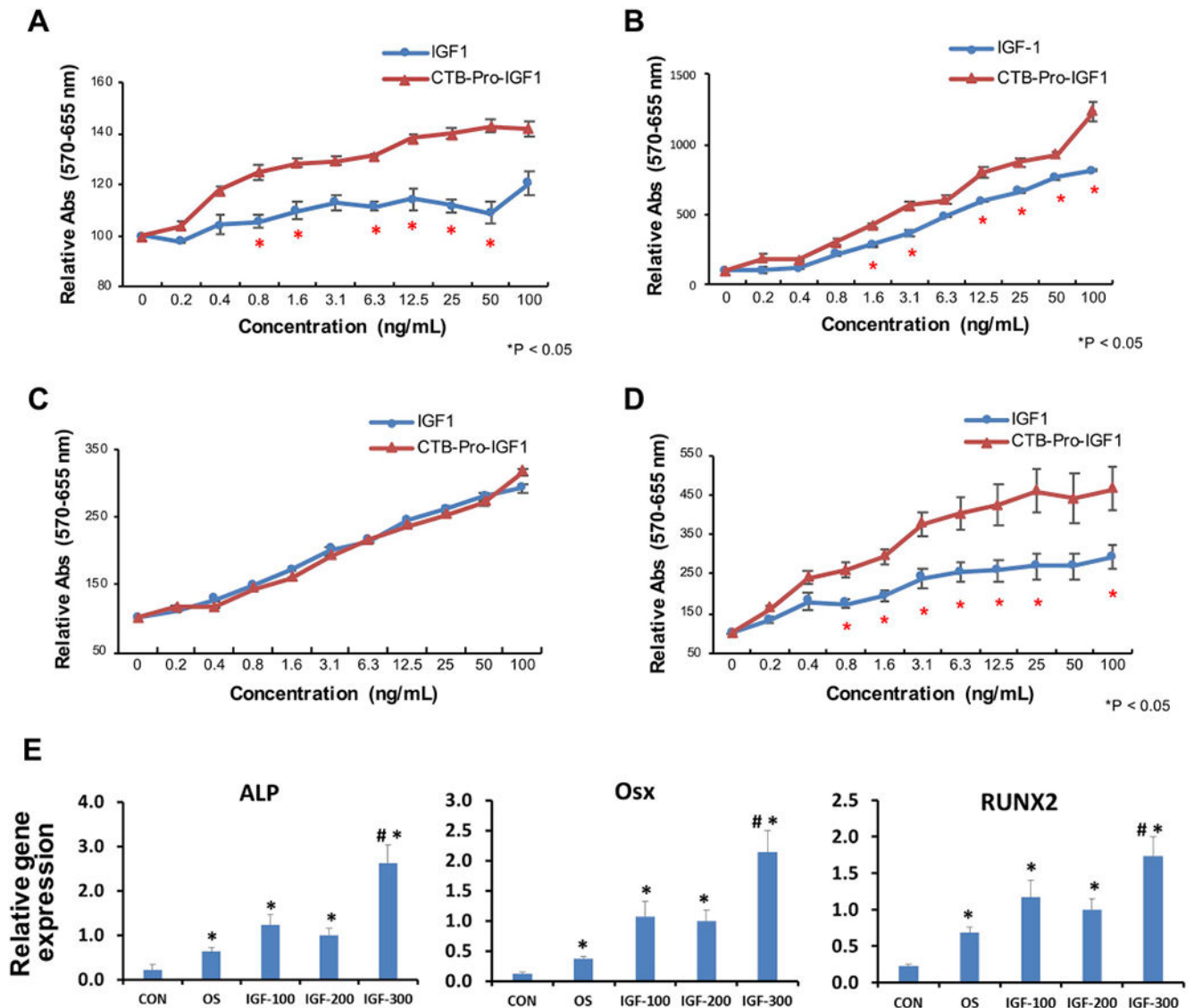


**Fig. 4. CTB-Pro-IGF-1 promotes keratinocyte, MSCs and osteoblast cell proliferation and osteoblast differentiation.**

(A-D) Relative absorbance of viable (A) HOK (Human Oral Keratinocytes), (B) GMSCs (Human Gingiva derived Mesenchymal Stromal Cells, MSCs), (C) SCCs (Human head and neck Squamous Carcinoma Cells), and (D) MC3TC (Mouse Osteoblast Cells) after incubation with purified CTB-Pro-IGF-1. IGF-1 peptide was utilized as positive control. The data is representative of two biological repeats run in triplets. Data are expressed as the mean  $\pm$  SEM. \* indicates P-value < 0.05 vs. IGF-1 by ANOVA. (E) qPCR analysis of osteogenesis marker genes. ALP, Alkaline Phosphatase; RUNX2, Runt related transcription factor 2; Osx, Osterix. Mouse osteoblastic cell line MC3T3 was induced in osteogenic media (OS) with 100 ng/ml (IGF-100), 200 ng/ml (IGF-200) and 300 ng/ml (IGF-300) of purified CTB-Pro-IGF-1 for 5 days. CON, MC3T3 cells in growth media; OS, MC3T3 cells in osteogenic media. \* indicates P < 0.05 vs. CON and # indicates P < 0.05 vs. OS.

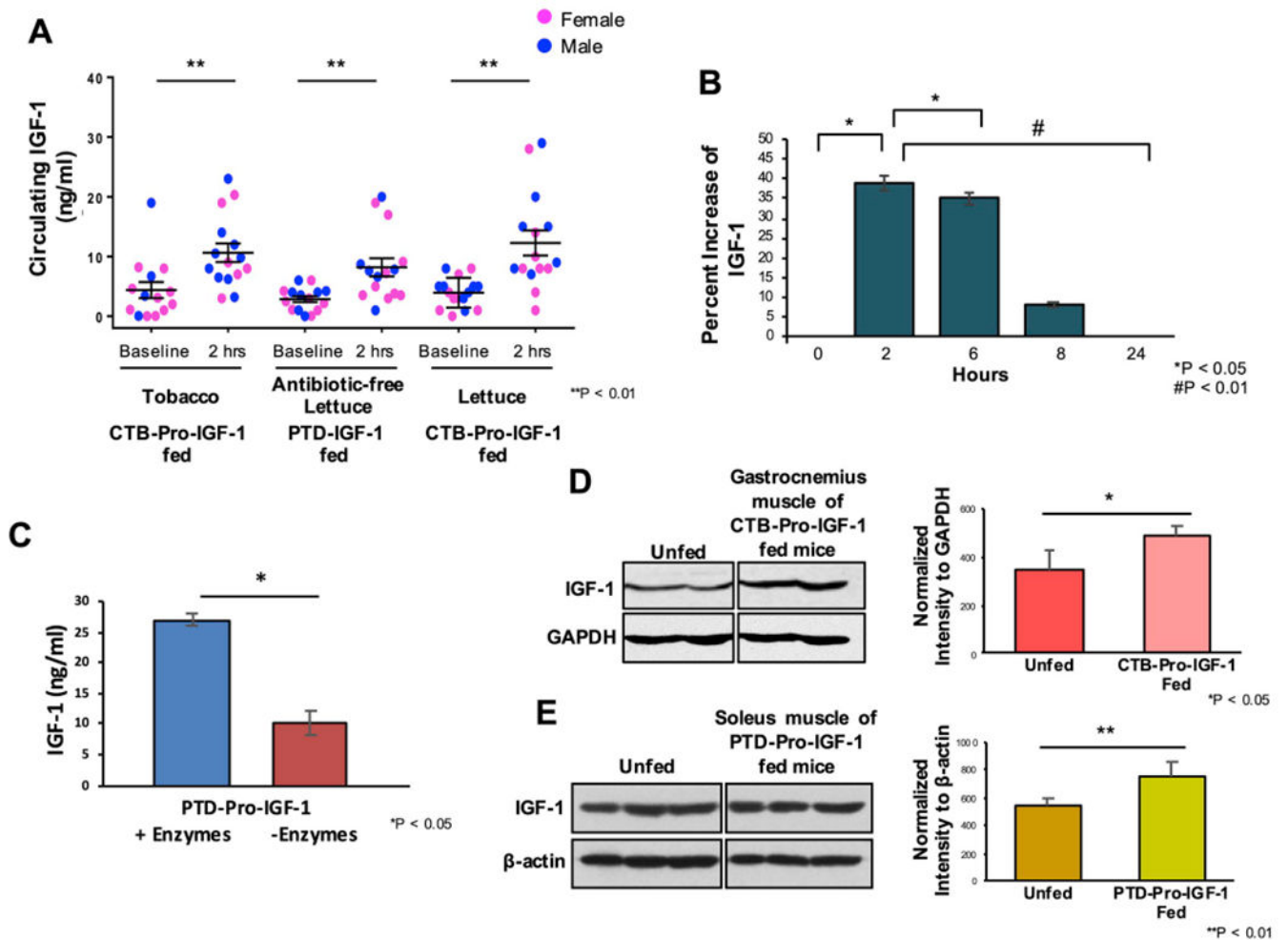


**Fig. 5. Characterization of oral Delivery of CTB-Pro-IGF-1 and PTD-Pro-IGF1.**

(A) Absorption of IGF-CHK-1 in sera at 2 h after oral gavage. C57BL/6J mice (n=14 to 16 mice per group) were fed with lyophilized cells containing 5  $\mu$ g dose of CTB/PTD-IGF-1. Data points represent individual male (blue dots) or female (pink dots) mice. \*\* P-value < 0.01. (B) Kinetic analysis of CTB-Pro-IGF-1 in plasma over 24 h (n = 6). Data are shown as % change  $\pm$  SEM. \*P < 0.05 and #P < 0.01 by ANOVA. (C) Release of PTD-Pro-IGF-1 from intact plant cells in vitro in the presence or absence cell wall degrading enzymes (mannanase, pectinate lyase, endoglucanase, exoglucanase) expressed in plant cells. Mean  $\pm$  SEM. \*P < 0.05 by *t*-Test. (D) IGF-1 levels in gastrocnemius muscle at 5 h after oral administration of CTB-Pro-IGF-1 (left) as determined by densitometric quantitation of western blots, with GAPDH as an internal loading control (right). Mean value  $\pm$  SEM. \* indicates P-value < 0.05 vs. unfed by ANOVA. (E) IGF-1 levels in soleus muscle at 5 h after oral administration of PTD-Pro-IGF-1 as determined by immunoblot against anti-IGF-1 (left), after normalization to  $\beta$ -actin (right). Mean value  $\pm$  SD. \*\* indicates P-value < 0.01 vs. unfed by ANOVA. (For interpretation of the references to colour in this figure legend, the reader is referred to the Web version of this article.)

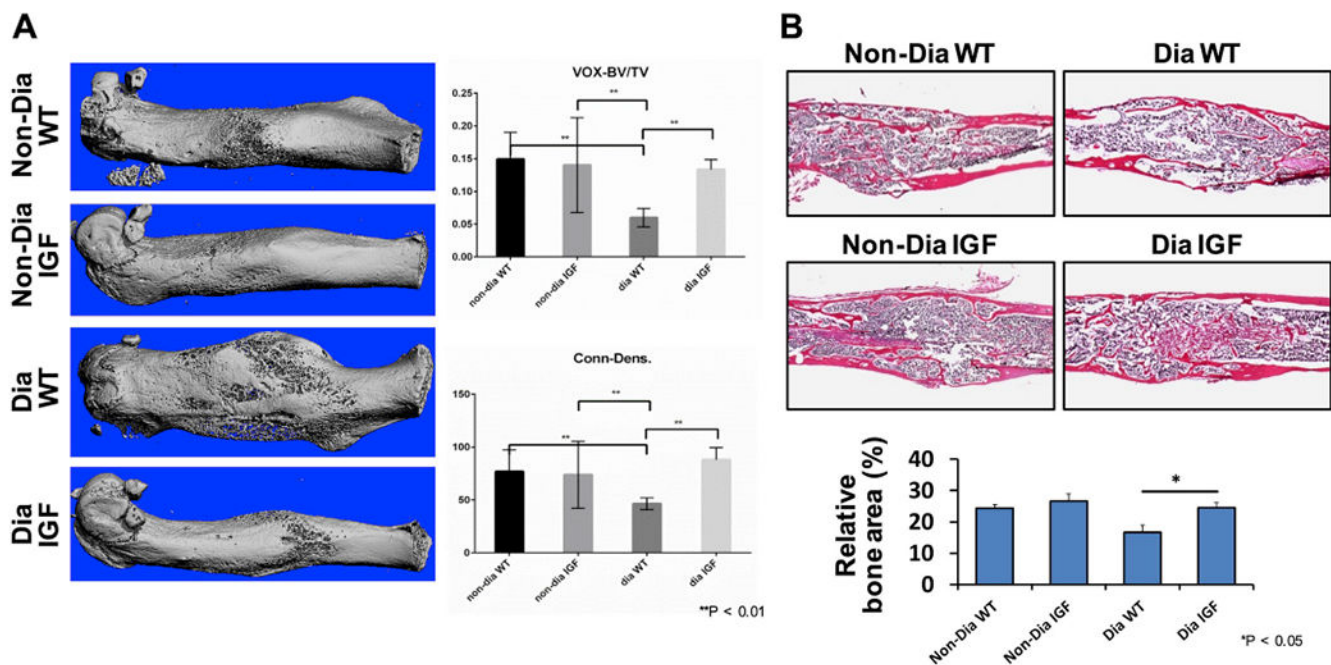


**Fig. 6. Oral administration of CTB-Pro-IGF-1 promotes bone regeneration in diabetic fracture healing.**

(A) Representative images of 3-D re-constructions from sections of micro CT scan in the fracture area at 6 weeks post fracture (right). Quantitative measurements of newly formed bone at the fracture gap (right). BV/TV, bone volume fraction; Conn-Dens, connectivity density. (B) Histological analyses (top) and relative bone area (bottom) for each group. Data are expressed as the mean  $\pm$  SEM. \*P < 0.05 between groups. \*\*P < 0.01 between groups. Non-Dia WT group (non-diabetic mice, oral gavaged with lyophilized wide type plant cells), Non-Dia IGF group (non-diabetic mice, oral gavaged with lyophilized plant cells containing CTB-Pro-IGF-1), Dia WT group (diabetic mice, oral gavaged with lyophilized wide type plant cells), Dia IGF group (diabetic mice, oral gavaged with lyophilized plant cells containing CTB-Pro-IGF-CHK-1).